Using remote sensing to detect indicator species of tidal influence along the lower Apalachicola River, Florida

by

Eian Margaret Davis

A thesis submitted to the Graduate Faculty of
Auburn University
In partial fulfillment of the
Requirements for the Degree of
Natural Resources, Master of Science

Auburn, Alabama
May 6, 2023

Coastal Wetlands, Apalachicola, Imagery Analysis, Change Detection, *Sabal palmetto*, *Juncus roemerianus*

Approved by

Christopher Anderson, Co-chair, Professor, Natural Resources Management
Lana Narine, Co-chair, Assistant Professor, Geospatial and Environmental Informatics
Stephanie Rogers, Assistant Professor, Department of Geosciences

Abstract

Wetlands are an important part of coastal ecosystems for the multiple services they provide, including erosion control, water quality, and wildlife habitat. With the threat of rising sea levels, it is important to understand the potential shifts in these ecosystems for the services they provided and for the overall health of the environment. Apalachicola Bay is one of the most productive coastal systems in the southeastern United States (U.S.). Important shifts in freshwater input to the bay and lower Apalachicola River have been caused by managed flows in the watershed, recent and significant droughts, and climate change. Studying wetlands along the Apalachicola River, the primary objectives of this work were to: (1) understand the range of the tidal freshwater forested wetlands along the lower Apalachicola River based on the detection of cabbage palm (*Sabal palmetto*) using image classification of National Agriculture Imagery Program (NAIP) imagery, and (2) analyze shifts in tidal herbaceous vegetation through a time series image analysis using black needlerush (*Juncus roemerianus)*. Both species are understood to be important indicator species of tidal conditions along the lower river. Though the extent of cabbage palm within the study area was greater than expected, the detection of this species showed patterns of occurrence primarily along river ways and along the transitional zone between forest and marshland, Results suggest tidal influence may occur further inland that expected. Based on a 14-year change detection of *Juncus* marsh, 2008-2014 experienced more gain (596.3 hectares) than loss (114.7 hectares), but the opposite was found in the years between 2014-2022 (157.8 hectares of gain, 371.4 hectares of loss). These results indicate that relative river flow and its control of the lower river salinity may play a role in the distribution of cabbage palm and changes in marsh composition. By better understanding the range of tidal influence

along the Apalachicola River, findings from this study will aid resources managers in identifying and mitigating current and future wetland composition shifts.

Acknowledgements

Appreciation for the funding in support of my research and my graduate assistantship provided by the Apalachicola National Estuarine Research Reserve, the Florida Department of Environmental Protection, and the Auburn University College of Forestry, Wildlife and Environment.

I am deeply grateful for the patience and kindness of Dr. Christopher Anderson and Dr. Lana Narine through this study, and for inviting me to participate in this unique experience. GIS analysis and the natural world have always been a passion of mine and I greatly appreciate this opportunity I was giving. The journey was long, but their encouragement and guidance inspired me more than I could have ever hoped. Before I began my graduate education, I received my undergraduate degree at Auburn University where I first met Dr. Anderson in a sample techniques class which is what first started my pursuit of knowledge on wetland ecosystems and my passion to protect these beautiful resources. Dr. Anderson, thank you for the many opportunities you have given me over the years. Over these last two years, I have learned much from Dr. Narine on GIS and remote sensing practices that I will carry with me through my career. Thank you so much for your guidance.

Thank you to Dr. Stephanie Rogers for agreeing to be on my committee and pushing me to be a better researcher. She not only taught me, but she inspired me to dig deep for the fireworks in science and in my life. Thank you to Seamus White and James Fukai for their help in overcoming computer and software challenges throughout this experience.

I am eternally grateful for my dear friends Andrew Johnson and Kristen Parker. Through the bad times and the good, they always believed in me and were never afraid to say it. Though it may seem small to some, your generosity and friendship has been a beacon of light in some of my darkest times. Thank you both.

Finally, special thanks to my parents, John Mark and Stacy Davis. Without these two amazing people, I would not be where I am today, and I hope I continue to make them proud on my next journey in life.

Table of Contents

Table of Tables

Table of Figures

Chapter 1: Introduction

1.1 Background

Wetlands are an important feature of many landscapes in the U.S. and are among the more productive ecosystems in the world (United States Environmental Protection Agency, 2021). Wetland ecosystems provide multiple ecosystem services that are vital to humanity and wildlife such as nutrient cycling, flood protection, shoreline erosion control, and habitat for native species (Barbier et al. 2011; United States Environmental Protection Agency, 2021; Blankespoor et al., 2014). Wetlands are characterized by three distinct features: hydric soils, hydrophytic vegetation, and saturated or inundated conditions through a at least a portion of the growing season (United States Environmental Protection Agency, 2013). Coastal wetlands cover approximately 40 million acres and make up 38% of all wetland area in the conterminous USA (United States Environmental Protection Agency, 2021). Coastal wetland systems are an important asset to fisheries and environmental services around the globe. Though many steps have been taken to protect these resources, they are still threatened by many outside forces. Human activities such as drainage, dredging, construction, and pollution are just a few challenges faced by these ecosystems and their resource managers today (United States Environmental Protection Agency, 2013). The stability of these tidal wetland ecosystems is also threatened by climate change effects, sea level rise and human activity such as river management and pollution (Kirwin & Megonigal, 2013).

The Apalachicola Bay region in western Florida (Figure 1) is an important system of hydrological and ecological significance. The lower Apalachicola River and Apalachicola Bay are a large coastal outlet for three major rivers in the Southeastern United States: the Apalachicola, Chattahoochee, and Flint Rivers. This watershed covers 48,500 km^2 through

western Georgia, southeastern Alabama, and north Florida (Livingston, 1991). Research has been carried out in this region for a multitude of purposes to help provide better management of estuarine productivity, water quality, and biodiversity (Livingston, 1991). Understanding and managing this region is crucial because of a historically important fishery in the bay and the variety of stressors that can impact the stability of its ecosystems. Salinity along the coast, nutrient flux from agriculture, forestry activity, pesticides, marine pollution, etc. all have an impact of the stability and production of coastal ecosystems. Moving up the river, riparian wetlands transition gradually from tidal marsh to tidal and non-tidal forested wetlands as they move inland along the Apalachicola River (Anderson & Lockaby, 2011). Concerns about reduced flows and their effect on saltwater intrusion into forested wetlands are important because they can eventually increase tree mortality or/and overall shifts in community composition (Anderson et al., 2013; DeSantis et al., 2007; Zhai et al., 2018) and weaken the resilience of these ecosystems.

Human impact on coastal water quality and hydrological patterns has been seen all over the globe, from activities such as agricultural runoff and river management. These activities impact the health of the native species in the area as well as species in the lower watersheds. This was seen in Apalachicola Bay in 2012 when there was a crash in oyster production due to various human and environmental pressures (Elliott, 2020). Since then, the oyster fishery in Apalachicola Bay has been under pressures from other stressors as well, such as the Deepwater Horizon oil disaster (2010), Hurricane Michael (2018), and changes to freshwater flow from upstream rivers (Elliott, 2020). The freshwater input to Apalachicola Bay has been a contentious issue for Georgia, Florida, and Alabama over several decades as the states began to dispute water flow from the basin.

The overall goal of this study was to identify potential shifts in the wetland composition along the lower Apalachicola River and Bay related to tidal influence. Earth Observation (EO) data offers powerful capabilities for visualizing large areas and allows for environmental monitoring over an extended period. Using aerial and satellite imagery, this project will aid in informing land managers in the Apalachicola region of changes in the wetland environment as well as estimating tidal/non-tidal boundaries. Also, this work developed methods for detecting coastal wetland communities using geospatial techniques. These methods could prove useful in planning and mitigating against shifts in climate, potential risk posed by sea level rise (SLR), and human impacts to environmental inputs. Due to relatively low slope and elevation, this area is vulnerable to SLR and damage from intensified storms and other natural hazards due to climate change.

1.2 Review of Relevant Literature

Coastal wetlands include salt marshes, tidal freshwater wetlands (both marsh and forested), and mangroves that can occur over a range of salinities and hydrological conditions. Distinctions between freshwater tidal versus inland wetlands are not clear-cut due to the gradient of biophysical conditions as proximate to the coastline increases. Approximately 60% of coastal salt and freshwater marshes in the United States are found along the coastal plain along the Gulf of Mexico (Mitsch and Gosselink, 2015). These wetlands can be found in narrow fringes along steep shorelines, near river mouths, in bays, on coastal plains, and around lagoons from Maine to Florida and on to Louisiana and Texas. In coastal marshes found adjacent to large rivers, like the Apalachicola River, freshwater inputs aid in diluting salinity from the bay or estuary and create brackish or sometimes even freshwater conditions (Mitsch and Gosselink, 2015). Tidal freshwater wetlands receive the same nutrient and flooding as a salt marsh without the salt stress.

Tidal freshwater forested wetlands (TFFWs) are no exception. Some of the most extensive TFFWs found in the United States occur along the southeastern coastline (Mitsch and Gosselink, 2015). Though the lower extent of TFFWs is typically bordered by marsh, the upper extent becomes unclear has the wetlands transition to non-tidal conditions.

Remotely sensed imagery from different source has been used in numerous studies to assess wetland communities in order to gain a better understanding of the species distribution and/or patterns of hydrology and vegetation composition (Baker et al. 2006; Correll et al. 2019; Lossou et al. 2019; Zhang et al. 2020). For example, NAIP (National Agriculture Imagery Program) provides high spatial resolution (1-meter) aerial imagery that was used by Correll et al (2019) to map the zonation of coastal plant communities in Maine and Virginia, USA while Waldron et al (2021) used NAIP to determine the effects of sea level rise on coastal marshes along the Pascagoula River in Mississippi, USA. Another common image source used is Landsat satellite imagery. Baker et al (2006) used multi-seasonal Landsat imagery along with ancillary data to map wetland and riparian areas within the Gallatin Valley in southwest Montana, USA. Given the long, continuous archive of imagery provided by the Landsat program (Wulder et al., 2008), Landsat imagery has been utilized in several studies in order to perform times series assessments of salt marshes (Sun et al. 2018; Lopes et al. 2020; Campbell and Wang, 2020; Zhang et al 2020) and tropical forests (Lossou et al 2019).

The image classification method chosen for this study is the Maximum Likelihood classifier (MLC) and has been adopted for many ecosystem assessments (Chust et al. 2008; Xie et al. 2019; Lossou et al. 2019; Waldron et al. 2021; Liang et al. 2022). MLC has been used for forested land cover classifications (Xie et al. 2019; Lossou et al. 2019; Liang et al. 2022), habitat mapping (Chust et al. 2008; Anderson et al 2016), and salt marsh classification (Waldron et al.

2021). Xie et al. (2019) also found that performance of the MLC improved for forest class types when imagery is taken in the leaf-off season in Kelaqin, Inner Mongolia, China.

1.3 Apalachicola Estuary

The Apalachicola River corridor is considered an area with one of the highest levels of biodiversity in North America, supporting upwards of 40 species of amphibians and 80 species of reptiles alone (Florida Natural Areas Inventory, 2005). Apalachicola Bay is also a historically important aquatic system for oyster production in the state of Florida as well as a major nursery for blue crab and marine fishes (Florida Fish and Wildlife Conservation Commission, 2021). Both the Apalachicola River and Bay can be seen in Figure 1. The area of interest (AOI) of this study, which includes the entire tidal reach of the lower river and riparian wetlands, is a total area of 28,732 ha (Figure 1). This is an important area for conservation of natural resources in terms of impacts from human activity and shifts in climatic conditions.

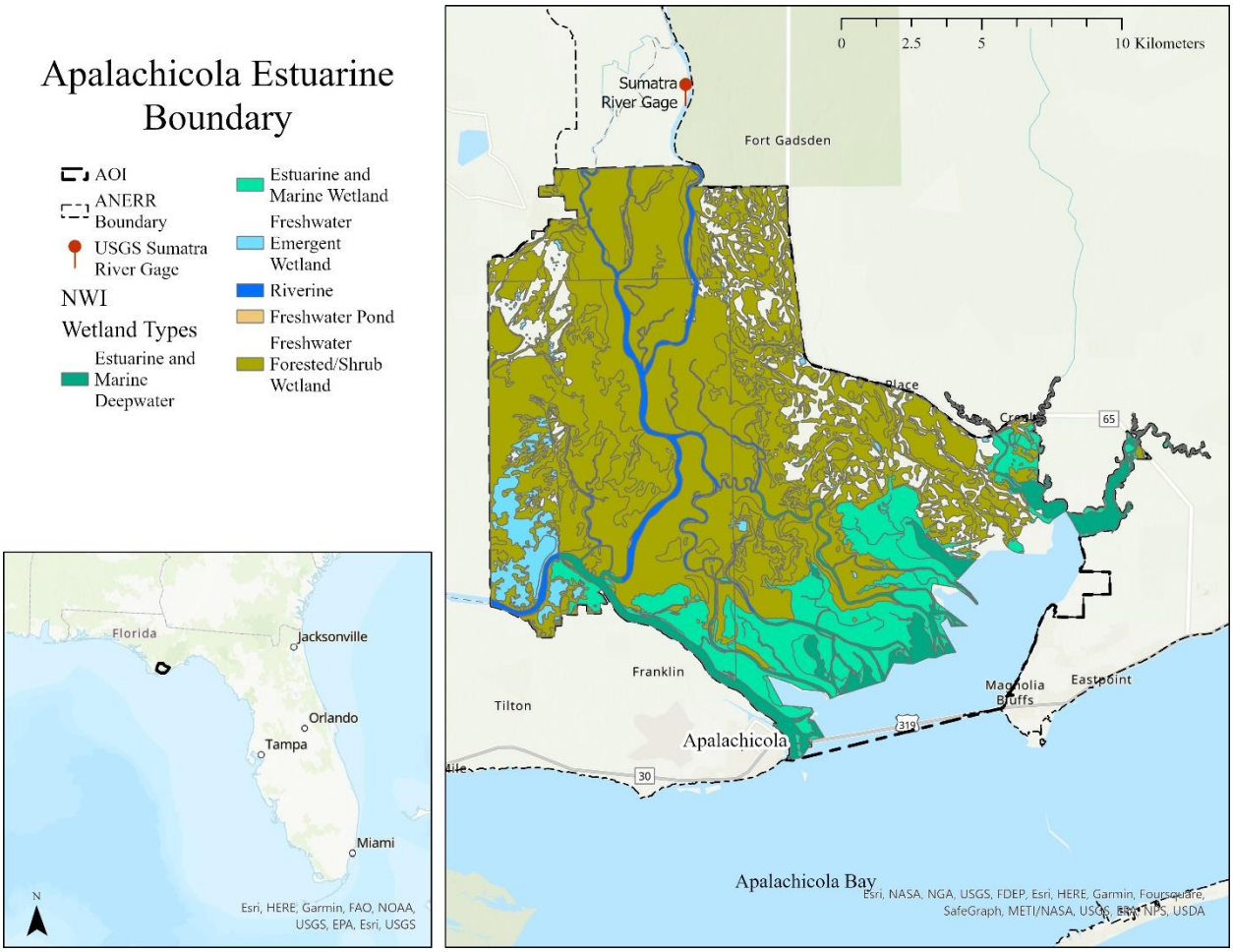

Figure 1. The Apalachicola Estuary area of interest (AOI). This map represents the location of the Apalachicola National Estuarine Research Reserve (ANERR) along the Gulf Coast of Florida. Wetland Classification types from the National Wetland Inventory (U.S. Fish and Wildlife Service, 2022).

The lower Apalachicola River floodplain and surrounding territory has a flat topography and gradual slope. It drains to Apalachicola Bay which is delineated by barrier islands (St George and St Vincent Islands) along the outer reach of the bay. Flooding is more likely to occur along the river floodplain during large influx of water whether it be storm induced or gradual increase in the water table through higher river flows in the winter. As seen in Figure 2, this area has an extensive hydrological network of streams and rivers. The Apalachicola River is also among the largest rivers in the Southeast U.S. in terms of flow and the Apalachicola River floodplain is the largest in the state of Florida (Ward et al., 2005). Based on the annual average

discharge data from the USGS Sumatra monitoring gage (Water Resources Data, n.d.) from 1978 to 2021, the Apalachicola River discharge ranged from 9,715 to 36,860 cubic feet per second.

The main types of soil found along the lower river floodplain are Bohicket and Tisonia soil (silty clay, very poorly drained) and Chowan, Brickyard and Kenner soil (silty clay loam, very poorly drained) (USDA Natural Resource Conservation Service, n.d.). Soils containing clay (common in the region) are also more prone to flooding versus the more porous sandy soils due to the lower hydraulic conductivity of loamy, clay soils. This soil type causes more water to remain on the landscape during rain/flood events, causing floodplain conditions. With such a large floodplain running through the AOI and through the Apalachicola estuary, the area produces conditions for extensive riparian wetlands (woody or freshwater forested/shrub wetland types).

Tidal influence is important for many of our coastal wetlands and should be considered when classifying wetlands, especially in specific types (such as freshwater swamp versus tidal marsh). The tides of Apalachicola Bay are considered microtidal (typically <1.0 m range) and have an alternating semi-diurnal and diurnal pattern (Doyle et al., 2007). In Figure 1, the six wetland types found in the AOI are seen: Estuarine and Marine Deepwater (5.6%), Estuarine and Marine Wetland (12.3%), Freshwater Emergent Wetland (2.7%), Freshwater Forested/Shrub (56.7%), Freshwater Pond (0.0%), and Riverine (2.7%) (Table 1). These wetland types were extracted from the National Wetland Inventory (NWI) provided by the U.S. Fish and Wildlife Service (2022). The description of each wetland type, the water regime subclass (saltwater tidal, freshwater tidal, or nontidal), and the total area for each type can be seen in Table 1. Percentages of wetland extent from the NWI are estimates and can contain arbitrary boundaries produced in the mapping process due to imagery boundaries, resulting inaccuracies in the final product.

Table 1. Brief description of the AOI wetland types per National Wetland Inventory (U.S. Fish and Wildlife Service, 2022) and total area of each type in hectares.

Wetland Class	Brief Description	Water Regime	Area (Hectares)	Percent of Coverage
Estuarine and Marine Deepwater	Open water estuary, bay, sound, open ocean	Saltwater tidal	1,619.7	5.6%
Estuarine and Marine Wetland	Vegetated and non-vegetated brackish and saltwater marsh, shrubs, beach, bar, shoal or flat	Saltwater tidal	3,532.7	12.3%
Freshwater Emergent Wetland	Herbaceous marsh, fen, swale and wet meadow	Freshwater tidal	120.1	0.4%
		Nontidal	649.3	2.3%
Freshwater Forested/Shrub	Forested swamp or wetland shrub bog or wetland	Freshwater Tidal	3,014.6	10.5%
		Nontidal	13,275.0	46.2%
Freshwater Pond	Pond	Freshwater Tidal	5.8	0.0%
		Nontidal	7.4	0.0%
Riverine	River or stream channel	Freshwater Tidal	465.8	1.6%
		Nontidal	315.5	1.1%
Total			23,005.9	80.1%

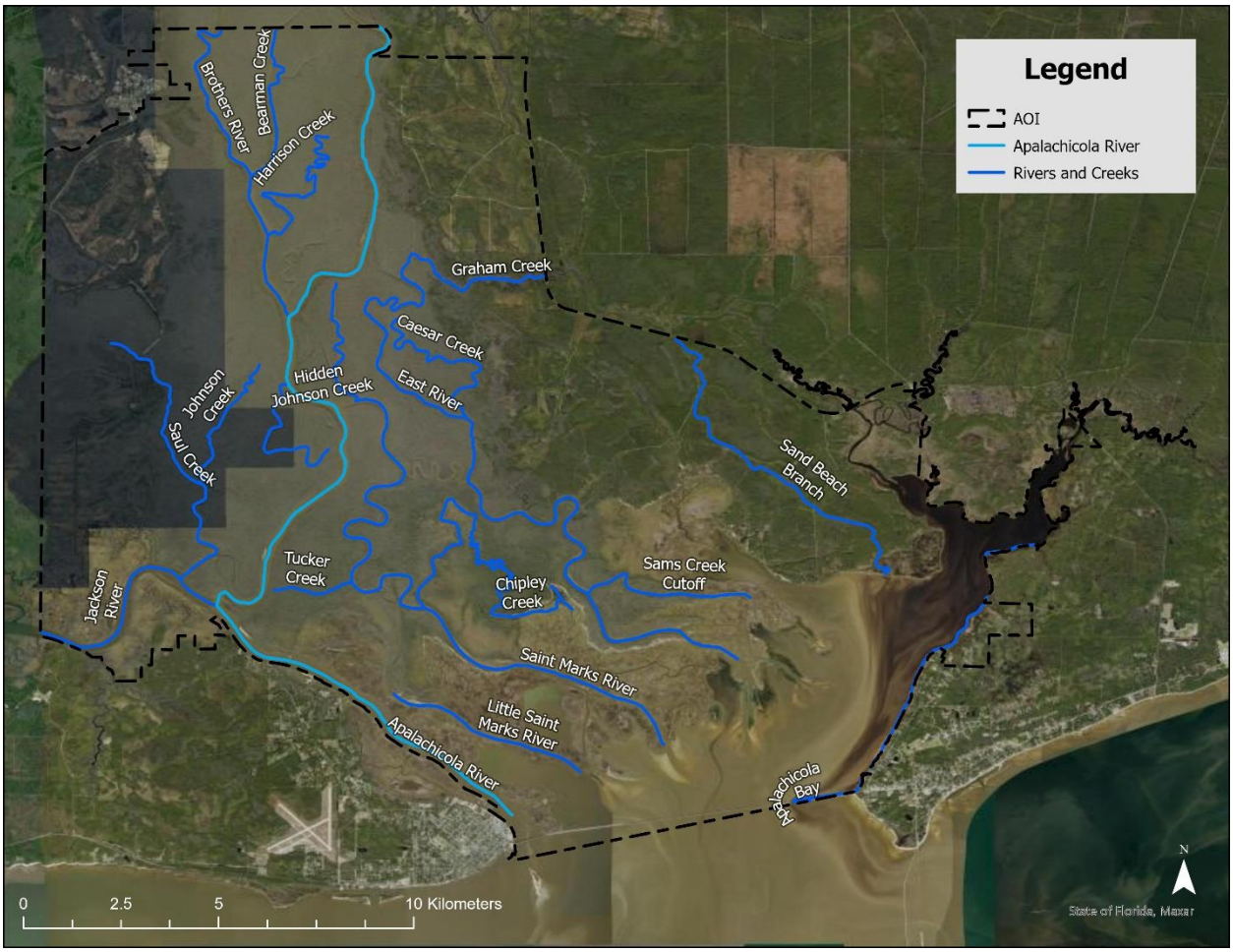

Figure 2. Main rivers and drainages inside the AOI.

1.4 Objectives

The primary objectives of this project were to: (1) identify an approximate tidal/non-tidal forested wetland boundary by mapping the spatial extent of cabbage palm (an indicator species of tidal influence) and, (2) identify potential shifts in the extent of brackish marshes at the mouth of the Apalachicola River by mapping the spatial extent of black needlerush (*Juncus roemerianus*) (an indicator species for moderate marsh salinity) from 2008-2014 and 2014-2022. The first objective focuses on the freshwater forested/shrub wetland and riverine type (56.7% of wetland in the AOI) and the second objective focuses on the three marsh types- estuarine and marine deepwater and wetland, and freshwater emergent wetland (20.6% of wetland in the AOI).

With impacts from water management and the threat of SLR continuing, it is important to document and monitor changes that occur to these wetland ecosystems for future generations and land management practices.

Each primary objective was examined through a study presented as a separate chapter of the thesis. Objective 1 is presented in Chapter 2 of the thesis; Chapter 3 addresses Objective 2; and Conclusions and Recommendations are presented in Chapter 4**.**

References

Anderson, C. J., & Lockaby, B. G. (2011). Forested Wetland Communities as Indicators of Tidal Influence along the Apalachicola River, Florida, USA. *Wetlands*(31), 859-906. doi:https://doi.org/10.1007/s13157-011-0204-5

Anderson, C. J., Lockaby, B. G., & Click, N. (2013). Changes in Wetland Forest Structure, Basal Growth, and Composition across a Tidal Gradient. *The American Midland Naturalist, 170*(1), 1-13. doi:10.1674/0003-0031-170.1.1

Baker, C., Lawrence, R., Montagne, C., & Patten, D. (2006). Mapping Wetlands and Riparian Areas Using Landsat ETM+ Imagery and Decision-Tree-Based Models. *WETLANDS, 26*(2), 465-474.

Barbier, E. B., Hacker, S. D., Kennedy, C., Koch, E. W., Stier, A. C., & Silliman, B. R. (2011). The value of estuarine and coastal ecosystem services. (A. M. Ellison, Ed.) *Ecological Monogrpahs, 81*(2), 169-193. Retrieved from https://doi.org/10.1890/10-1510.1

Blankespoor, B., Dasgupta, S., & Laplante, B. (2014). Sea-Level Rise and Coastal Wetlands. *AMBIO, 43*(8), 996-1005. doi:10.1007/s13280-014-0500-4

Brooks, K. N., Ffolliott, P. F., & Magner, J. A. (2013). Hydrology and the Management of Watersheds (Fourth ed.). *Wiley-Blackwell.*

Campbell, A. D., & Wang, Y. (2020). Salt Marsh monitoring along the mid-Atlantic coast by Google Earth Engine enabled time series. *PLoS ONE, 15*(2). doi:10.1371/journal.pone.0229605

Celik, S., Anderson, C. J., Kalin, L., & Rezaeianzadeh, M. (2020). Long-term Salinity, Hydrology, and Forested Wetlands Along a Tidal Freshwater Gradient. *Estuaries and Coasts*. doi:10.1007/s12237-021-00911-8

Chust, G., Galparsoro, I., Borja, Á., Franco, J., & Uriarte, A. (2008). Coastal and estuarine habitat mapping, using LiDAR height and intensity and multi-spectral imagery. *Estuarine, Coastal and Shelf Science, 78*(4), 633-643. Retrieved from https://doi.org/10.1016/j.ecss.2008.02.003

Correll, M. D., Hantson, W., Hodgman, T. P., Cline, B. B., Elphick, C. S., Shriver, W. G., Shriver, G., Tymkiw, E. L., and Olsen, B. J. (2019). Fine-Scale Mapping of Coastal Plant Communities in the Northeastern USA. *Applied Wetland Science,* 39, 17-28. doi:10.1007/s13157-018-1028-3

DeSantis, L. R., Bhotika, S., Williams, K., & Putz, F. E. (2007). Sea-level rise and drought interactions accelerate forest decline on the Gulf Coast of Florida, USA. *Global Change Biology, 13*(11), 2349-2360. doi:10.1111/j.1365-2486.2007.01440.x

Doyle, T. W., O'Neil, C. P., Melder, M. P., From, A. S., & Plata, M. M. (2007). Tidal Freshwater Swamps of the Southeastern United States: Effects of Land Use, Hurricanes, Sea-level

Rise, and Climate Change. *Ecology of Tidal Freshwater Forested Wetlands of the Southeastern United States*. doi:10.1007/978-1-4020-5095-4_1

Elliott, D. (2020). Florida Closes Iconic Apalachicola Oyster Fishery. *NPR: National*. Retrieved from https://www.npr.org/2020/07/22/894074674/floridas-oyster-beds-devastated-by-years-of-drought-other-pressures

Fagherazzi, S., Anisfeld, S. C., Blum, L. K., Long, E. V., Feagin, R. A., Fernandes, A., . . . Williams, K. (2019). Sea Level Rise and the Dynamics of the Marsh-Upland Boundary. *Frontiers in Environmental Science, 7*(25). doi:10.3389/fenvs.2019.00025

Florida Fish and Wildlife Conservation Commission. (2021). *Apalachicola River - Habitat and Management.* Tallahassee, FL: Florida Fish and Wildlife Conservation Commission. Retrieved from https://myfwc.com/recreation/lead/apalachicola-river/habitat/

Florida Natural Areas Inventory. (2005). *Biology: Plants, Animals, & Habitat - We live in a hot spot of biodiversity.* Florida . Tallahassee, FL: ARROW. Retrieved from https://www.fnai.org/ARROW/Almanac/biology/biology_index.cfm

Khojasteh, D., Glamore, W., Heimhuber, V., & Felder, S. (2021). Sea level rise impacts on estuarine dynamics: A review. (J. Gan, Ed.) *Science of the Total Environment, 780*, 146470. Retrieved from https://doi.org/10.1016/j.scitotenv.2021.146470

Kirwan, M. L., & Megonigal, J. P. (2013). Tidal wetland stability in the face of human impacts and sea-level rise. *Nature, 504*(7478), 53-60. doi:10.10038/nature12856

Wulder, M.A., White, J.C., Goward, S.N., Masek, J.G., Irons, J.R., Herold, M., Cohen, W.B., Loveland, T.R., and Woodcock, C.E. (2008). Landsat Continuity: Issues and opportunities for land cover monitoring. *Remote Sensing of Environment,* 112(3), 995-969. doi: 10.1016/j.rse.2007.07.004

Liang, F., Zhang, X., Li, H., Yu, H., Lin, Q., Jiang, M., & Zhang, J. (2022). Land Use Classification Based on Maximum Likelihood Method. *Advances in Intelligent Data Analysis and Applications*, 133-139. doi:10.1007/978-981-16-5036-9_15

Livingston, R. J. (1984). *The ecology of the Apalachicola Bay system: an estuarine profile.* Washington, D.C.: U.S. Department of the Interior.

Livingston, R. J. (1991). Historical Relationships Between Research and Resource Management in the Apalachicola River Estuary. *Ecological Applications, 1*(4), 361-382.

Lockaby, B. G., Anderson, C. J., & Click, N. (2013). Chnages in Wetland Forest Structure, Basal Growth, and Composition across a Tidal Gradient. *The American Midland Naturalist, 170*(1), 1-13. doi:10.1674/0003-0031-170.1.1

Lopes, C. L., Mendes, R., Caçador, I., & Dias, J. M. (2020). Assessing salt marsh extent and condition changes with 35 years of Landsat imagery: Tagus Estuary case study. *Remote Sensing of Environmnet, 247*. doi:10.1016/j.rse.2020.111939

Lossou, E., Owusu-Prempeh, N., and Agyemang, G. (2019). Monitoring Land Cover changes in the tropical high forests using multi-temporal remote sensing and spatial analyses techniques. *Remote Sensing Applications: Society and Environment*, 16, 100264. doi: 10.1016/j.rsase.2019.100264

Mitsch, W. J., & Gosselink, J. G. (2015). *Wetlands* (Fifth ed.). Hoboken, New Jersey: John Wiley & Sons, Inc.

Sun, C., Fagherazzi, S., and Liu, Y. (2018). Classification mapping of salt marsh vegetation by flexible monthly NDVI time-series using Landsat imagery. *Estuarine, Coastal and Shelf Science*, 213, 61-80. doi: 10.1016/j.ecss.2018.08.007

USDA Natural Resources Conservation Service (n.d.). Web Soil Survey. Retrieved April 30, 2022, from https://websoilsurvey.nrcs.usda.gov/app/

U.S. Fish & Wildlife Service. (2022). *National Wetlands Inventory*. National Wetlands Inventory | U.S. Fish & Wildlife Service. Retrieved April 30, 2022, from https://www.fws.gov/program/national-wetlands-inventory

United States Environmental Protection Agency. (2013). *Wetlands - Status and Trends*. Retrieved from EPA: https://archive.epa.gov/water/archive/web/html/vital_status.html

United States Environmental Protection Agency. (2021). *Wetlands Protection and Restoration*. Retrieved from EPA: https://www.epa.gov/wetlands

Waldron, B., Claire, M., Carter, G. A., & Biber, P. D. (2021). Using Aerial Imagery to Determine the Effects of Sea-Level Rise on Fluvial Marshes at the Mouth of the Pascagoula River (Mississippi, USA). *Journal of Coastal Research, 37*(2), 389-407. Retrieved from https://doi.org/10.2112/JCOASTRES-D-20-00037.1

Ward, G. M., Harris, P. M., & Ward, A. K. (2005). Gulf Coast Rivers of the Southeastern United States. In A. C. Benke, & C. E. Cushing (Eds.), *Rivers of North America* (pp. 125-178). USA: Elsevier Academic Press.

Xie, Z., Chen, Y., Lu, D., Li, G., Chen, E. (2019). Classification of Land Cover, Forest, and Tree Species Classes with ZiYuan-3 Multispectral and Stereo Data. *Remote Sensing*, 11, 164. doi: 10.3390/rs11020164

Zhai, L., Krauss, K. W., Liu, X., Duberstein, J. A., Conner, W. H., DeAngelis, D. L., & Sternberg, L. d. (2018). Growth stress response to sea level rise in species with contrasting functional traits: A case study in tidal freshwater forested wetlands. *Environmental and Experiemnetal Botany, 155*, 378-386. Retrieved from https://doi.org/10.1016/j.envexpbot.2018.07.023

Zhang, X., Xiao, X., Wang, X., Xu, X., Chen, B., Wang, J., . . . Li, B. (2020, September). Quantifying expansion and removal of Spartina alterniflora on Chongming island, China, using time series Landsat images during 1995–2018. *Remote Sensing of Environment, 247*, 111916. doi:10.1016/j.rse.2020.111916

Chapter 2: Mapping an indicator species of tidal freshwater forested wetlands along the Apalachicola River, Florida, USA

Abstract

Wetlands are an important part of coastal ecosystems for multiple services they provide including erosion control, water purification, and wildlife habitat. Tidal freshwater forested wetlands (TFFWs) are an important but understudied part of deltaic systems in coastal areas around the world. Unfortunately, TFFWs, like other coastal wetlands, face threats due to climate change and river management but the upriver extent of these forests is often uncertain and difficult to predict. The primary goal of this study was to better understand the extent of TFFWs along the lower Apalachicola River, draining to Apalachicola Bay. Specific objectives were to: (1) detect an important indicator species (*Sabal palmetto* (cabbage palm)) for a TFFW community using high-resolution multispectral imagery and (2) develop a map product of the lower limit of this TFFW community using the indicator species. Utilizing National Aerial Imagery Program (NAIP) orthoimagery (blue, green, red, and near-infrared bands), a Maximum Likelihood image classifier was applied to detect cabbage palm. Additional input variables, including the Normalized Difference Vegetation Index (NDVI) and Near-Infrared (NIR) variance texture was then incorporated to assess potential improvements to classification accuracy. Mapped results showed that cabbage palm was common throughout the study area with several distinct ranges where it was dominant. Accuracy assessments of the classified images revealed that addition of NDVI alone caused a decrease in user accuracy from 63.8% to 56.1% for the Cabbage Palm class and a slight decrease in the overall accuracy (from 73.3% to 71.0%). When only the NIR variance band was incorporated with NAIP, the user accuracy was

the highest at 88.7% and the producer accuracy was 94.0%. When both the NDVI and NIR variance band were incorporated together, the user and producer accuracy were only slight lower than that of the NIR variance alone (80.0% and 92.0%, respectively). This suggests that NDVI has a negative effect on the detection of cabbage palm. Outcomes from this work can facilitate monitoring of TFFWs, promote informed mitigation practices, better understand the impact of salinity intrusion, and aid in planning for future land management in the face of sea level rise.

Key words: Coastal Wetlands, Freshwater Forested Wetlands, Imagery Analysis, *Sabal palmetto*

2.1 Introduction

Tidal wetlands consist of three main types: salt marshes, tidal freshwater wetlands (marsh and forest), and mangrove swamps (Mitsch & Gosselink, 2015). Tidal wetlands can occur over a range of salinities depending on proximity to freshwater and these variations support different communities. Understanding the extent of tidal influence is critical in natural resource assessment. Tidal freshwater forested wetlands (TFFWs) typically occupy the upriver extent of tidal influence and occur where riparian wetlands are flooded by primarily freshwater because of river flows. Under some conditions (low river flow), higher salinities may periodically occur. Understanding the extent of TFFWs will assist with planning related to sea level rise. Using age-distribution of cabbage palm and examination of patterns of tree species zonation in Waccassassa Bay State Preserve, Williams et al. (1999) found that exposure to salt seemed to have a major influence on the failure of coastal tree regeneration, but in high freshwater outlets (like Apalachicola), flooding stress potentially plays a larger role of regeneration failure of coastal forested wetlands. A study by Wang et al. (2022) found that it is highly likely that if these wetland types are impacted by salinity-intrusion, they could potentially lose some of their capacity to act as carbon sinks if up-slope migration does not occur. Another study found that salinity has a significant impact on forest community and structure, and that as salinity increases, the productivity of these ecosystems decreases (Liu, et al., 2017).

For this study, the TFFW composition of the lower Apalachicola River system in west-Florida, USA was investigated, specifically to determine an approximate tidal extent. Based on a previous study (Anderson and Lockaby, 2011), a few forested wetland species are indicative of tidal conditions throughout the lower Apalachicola River system (the mainstem and distributaries of the Apalachicola River). Anderson & Lockaby (2011) found two TFFW communities: 1)

swamp tupelo-bald cypress, and 2) cabbage palm-sweet bay. Tidal indicative species included: swamp tupelo (*Nyssa biflora),* Carolina ash *(Fraxinus spp.),* bald cypress *(Taxodium distichum),* and cabbage palm *(Sabal palmetto)*. Of all the species listed above, cabbage palm was the only species to be found strictly in the tidal freshwater forests, though it is not an indicator of all TFFWs. Although tidal conditions elicit a variety of physio-chemical conditions, salinity is commonly reported as an important factor for determining biotic communities. For instance, data from another study showed that areas dominated by TFFW indicator species in the lower Apalachicola River were found to have a 30-year daily-average salinity of >0.2 ppt, while plots with <0.2 ppt contained a more even mix of both non-tidal and tidal species and were considered transitional zones between the tidal and non-tidal forested wetlands (Celik et al., 2020).

Cabbage palm (*Sabal palmetto*) was observed as a reliable tidal wetland indicator along the lower Apalachicola River (Anderson & Lockaby, 2011; Celik et al., 2020) and is

Figure 1. Cabbage palm along the Apalachicola River edge in a TFFW within the study area. Taken by Eian Davis.

Figure 2. Aerial photo of cabbage palm stand.

distinguishable among the tree canopy in aerial imagery (<1 meter) due to its unique, circular fanned canopy structure. Individual cabbage palm specimens (Figure 1) can be

readily identified in aerial photographs (Figure 2). Cabbage palm has been documented elsewhere, persisting in tidally flooded areas in Waccasassa Bay Preserve State Park along the northern Gulf Coast of Florida for approximately 26 weeks, longer than other tidal wetland tree species (DeSantis et al., 2007), making it a good indicator species for TFFWs elsewhere. The native range for cabbage palm is throughout the southeastern United States, specifically Florida, coastal Georgia, South Carolina, Cuba, and the Bahamas (Zona, 1990). Cabbage palm can also be found in a range of community types: pinelands, swamps, mesic hardwood forests, and beachside dunes (Brown, 1973). Due to its evergreen status, its ability to persist within prolonged tidal flooding and its distinctive crown discernable in aerial imagery, cabbage palm was utilized to identify and estimate a tidal/non-tidal boundary in the coastal freshwater forested wetland communities in the lower Apalachicola River system.

Remote sensing and image classification have been used in a number of studies to assess land cover land use change and forest composition. In particular, the maximum likelihood classifier (MLC) has been shown to be effective at classifying forested land cover (Lossou, et al., 2019; Xie, et al., 2019; Liang, et al. 2022). One study done in Kelaqin, Inner Mongolia, China found that even though a higher accuracy could be achieved with support vector machine or random forest when classifying land cover types, MLC maintained a higher accuracy for forest type classification (76.43% - 89.41%) with images from leaf-off season (Xie et al., 2019). This study also found that the MLC had the highest accuracy for 4 out of 7 tree species detected, with the 4 all being pine or another conifer (Xie et al., 2019). Another study done on the Santa Genebra Forest in southeastern Brazil found that the use of a gray level co-occurrence matrix

(textural component) allows for species detection by enabling analysis of specific crown structures among the canopy (Ferreira et al., 2019).

The primary goal of this study was to approximate the extent of TFFWs along the Apalachicola River system in western Florida with a specific objective of detecting spatial distribution of *Sabal palmetto* for the tidal/non-tidal freshwater forested wetland community in Apalachicola. Using image classification approaches to detect cabbage palm and better understand the range of tidal forested wetlands, outputs from this work could be used by resource managers as a spatial reference for upriver tidal influence on the floodplains along the Apalachicola River system. Additionally, the outputs of this work highlight cabbage palm stands lining the upper limit of marshlands that could aid to monitor changes in the forest/marsh boundaries in the future.

2.2 Methodology

2.2.1 Study Area

The lower Apalachicola River and Apalachicola Bay is a large coastal outlet for three major rivers in the Southeastern United States: the Apalachicola, Chattahoochee, and Flint Rivers (Livingston, 1984). The area of interest for this study is the lower river systems which is approximately 27,876 ha within the Apalachicola National Estuarine Research Reserve (ANERR) (Figure 3). The large output of freshwater provided by the Apalachicola River (annual average: 674 cubic meters per second – USGS WaterWatch) combined with the influx of the coastal waters from the bay support a variety of wetland types.

According to the National Wetland Inventory provided by the U.S. Fish and Wildlife Service (2021), the main wetland types within the study area are: 20.6% estuarine and marine,

56.7% freshwater forested, and 2.8% freshwater pond/riverine. The freshwater forested wetland and riverine classes are further broken down by water regime of its zonation (U.S. Fish and Wildlife Service, 2021). Nontidal freshwater forested/shrub wetlands cover approximately 46.2% while 10.5% of the freshwater forested/shrub wetlands are designated as tidally influenced. The riverine wetland class has a nontidal zone of 320 ha and a freshwater tidal zone of 448 ha. There are no forested wetlands (including the riverine class) that are designated as saltwater tidal.

Figure 3. Location of the area of interest for this study (seen in red) within the Apalachicola National Estuarine Research Reserve (ANERR) along the lower Apalachicola River. The projection coordinate system for all datasets is NAD 1983 UTM Zone 16N.

2.2.2 Data

Imagery from the National Agriculture Imagery Program (NAIP) was utilized to complete this study. NAIP 1-m aerial imagery was retrieved from the U.S. Geological Survey. This imagery includes 4 spectral bands (Blue, Green, Red, and NIR). These data were chosen to identify cabbage palm trees along the canopy in imagery leaf-off season (fall or winter) for its fine spatial resolutions and open access. NAIP (1-meter resolution; 3-year temporal resolution) images data from December 2019 were used for analyses.

For the Cabbage Palm class, Geo-placemarks in Google Earth Pro were placed in known locations of cabbage palm (Christopher Anderson, personal communication, November 5, 2021). These areas were then reviewed through visual image interpretation techniques to confirm individual trees were selected for training and validation points. Additional locations of cabbage palms were identified through field observations made in December 2021 and later added to the geo-placemarks. Due the longevity of these target species (cabbage palm), confirmation of previously recorded cabbage palm (see Anderson and Lockaby, 2011) were revisited to validate the data used in the accuracy assessment. All areas with documented cabbage palm areas were verified on aerial imagery. Polygons representing the cabbage palm class were delineated based on single, visible tree crowns of the cabbage palm species. The same methods were applied for the Evergreen and Deciduous classes, where clearly visible treetops were delineated, with pine being the dominant species in the Evergreen class. The Herbaceous class is predominately marshland, with some pastures included. The Urban class represents all man-made structures and roads, and the Water class represents rivers, ponds, and the bay.

2.2.3 Data Processing

NAIP imagery was clipped to the extent of the study area and an unsupervised classification (ISODATA classification in ENVI) was performed to identify spectral profiles and to gain a better understanding of the area prior to an onsite visit. This assessment revealed 7 unique classes: water, urban, bare ground, pasture, herbaceous (marsh), forest, and shadows. For subsequent supervised classification, the classes were then revised to Herbaceous, Evergreen, Deciduous, Water, Urban, and Cabbage Palm. The purpose of using multiple classes was to identify which classes would have the most confusion with cabbage palm. Textural and vegetation indices (such as the Normalized Difference Vegetation Index – NDVI) have also been shown to aid in separation of classes among land cover type (Jeter & Carter, 2016; Waldron, et al., 2021). Textural indices (or texture) refer to the arrangement and frequency of variation in tone among pixels in a given image (Anys, et al. 1994; Hall-Beyer, 2016; Haralick, et al. 1973; Patel and Stonham, 1992; and Warner, 2011). For example, a rough surface or irregular structure among forest canopy (such as the one seen in cabbage palm, Figure 2) results in a rough texture, while landcover types like a pasture result in smooth textures (Anys, et al. 1994; Hall-Beyer, 2016; Haralick, et al. 1973; Patel and Stonham, 1992; and Warner, 2011). Textural variance is a measure of dispersion of values around the mean (Hall-Beyer, 2016) based on the greyscale quantization level (Anys, et al. 1994; Haralick, et al. 1973; Patel and Stonham, 1992; and Warner, 2011). In ENVI (L3Harris Geospatial Solutions, Inc., 2022), the textural layers for each band in the NAIP imagery was computed for variance, and a NDVI layer was computed in ArcGIS Pro (ESRI, 2022). NDVI uses the visible red band and the near-infrared band to create a vegetation greenness raster band. This index is useful for understanding and visualizing vegetation density and plant health (Vermote, et al., 2016; Masek, et al., 2006), and aids in

differentiating between evergreen forest species and deciduous species that would be dormant during the off-growing season (fall and winter). Below is the equation for the NDVI calculation:

$$NDVI = \frac{(Red - NIR)}{(Red + NIR)}$$

Three input datasets were generated using the new images: (1) variance for the near infrared (NIR) band stacked with the original (4-band) NAIP imagery, (2) NDVI and the original NAIP imagery, and (3) NIR Variance band (texture), the NDVI band, and the original NAIP imagery. For each of the 4 images, the supervised MLC in ArcGIS Pro (Liang, et al., 2022; Waldron, et al., 2021) was used. This process is visualized in the workflow below (Figure 4).

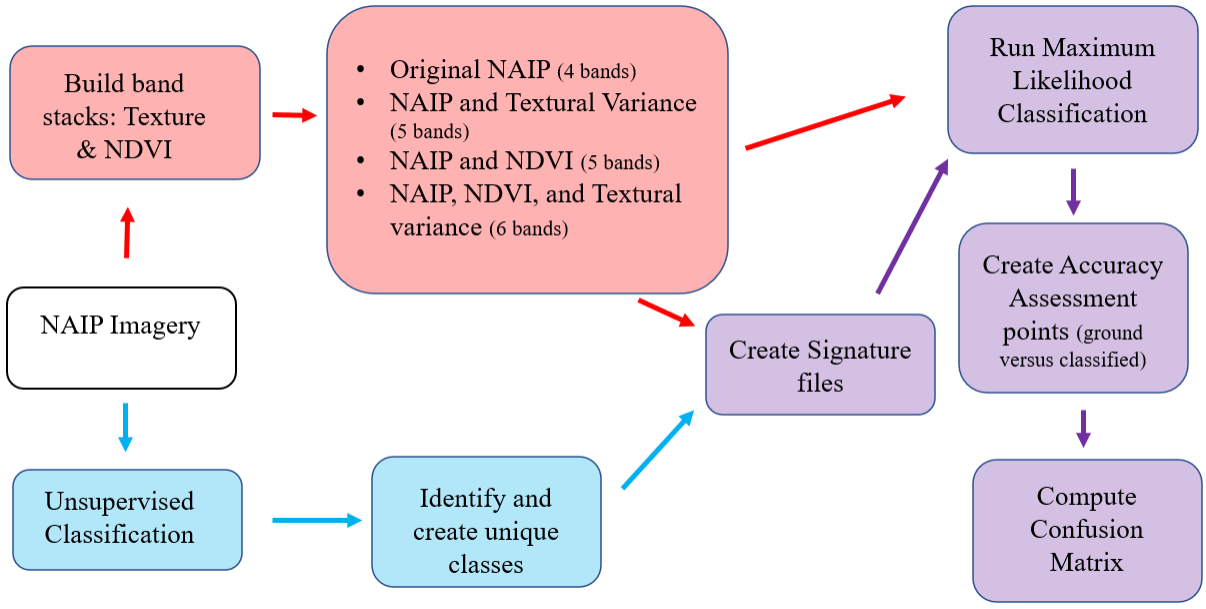

Figure 4. Workflow used for the Maximum Likelihood Classification of the NAIP imagery and two incorporated variables – Normalized Difference Vegetation Index (NDVI) and Texture (spatial variation of NIR greyscale level).

2.2.4 Classification Analysis

The MLC method was used to identify wetland communities through indicator species detection (cabbage palm) of the lower Apalachicola River system. Within the ANERR boundary, upland pine was observed, which was spectrally similar with the cabbage palm class. In order to limit potential confusion, the area of interest (AOI) (Figure 3) was delineated along the observed edge of the planted pine to exclude it from the classification process. Incorporating a textural component further addressed this issue by separating this land cover from the surrounding forested wetlands. The unique, linear pattern of the pine vegetation causes soil exposure between the trees, creating a unique change in tone between the image pixels allowing for the textural component to detect the change in pixel tones (Paine, 1981). Within the AOI boundary, MLC was performed on all 4 images: NAIP; NAIP & NDVI (NDVI); NAIP & Texture (Text); and NAIP, NDVI & Texture (N&T). Training data and validation (test) data inputs were the same for all classified images.

2.2.5 Validation of Classification Analysis

The accuracy of this analysis used data from past field studies (Anderson and Lockaby, 2011) and known locations of cabbage palm. All locations were verified based on clearly detectable cabbage palm in the high-resolution aerial imagery. The Create Accuracy Assessment, Update Accuracy Assessment, and Compute Confusion Matrix tools were used in ArcGIS Pro to perform the accuracy assessment of all classified images. The accuracy assessment points were created using a validation polygon shapefile for each class that had been previously verified. The validation polygon shapefile was created and verified through aerial image interpretations. The Create Accuracy Assessment tool was set to use the validation shapefile for ground truthing with 600 number of total test pixels with the same number of pixels (n=600) in each class (n=6) for all the confusion matrices (Figure 5). The confusion matrix for each MLC output was then used to

calculate the overall accuracy and kappa coefficient, and for each class, compute omission error, commission error, user accuracy and producer accuracy. The overall accuracy is the percentage of correctly classified values divided by the total number of test pixels (n=600). The kappa coefficient is a measure of agreement between the classified values and their respective true values beyond chance assignment, 1 represents 100% agreement and 0 represents no agreement. The user accuracy refers to the probability that a value was predicted to be in a class that it truly belongs to (correctly predicted values divided by the total number of values predicted). Producer accuracy is the probability that a value in a certain class was classified correctly. Commission errors refer to false positives in classes in the user accuracy, meaning values were predicted in a class in which they did not belong. A high commission error is a result of an overestimation of a class by the classification, or inclusion of values that are not the same as the ground truth. Omission errors refer to false negatives in the producer accuracy, meaning values that should have been predicted in a certain class were left out. A high omission error is the result of an underestimation of a class by the classification, or that ground truth points of class were excluded. After the accuracy assessments were performed, the cabbage palm class was extracted from the most accurate classified image and clipped to only show the distribution of cabbage palm in the Apalachicola River floodplain. A point density analysis was then performed to assess the density of cabbage palm pixels per hectare using ArcGIS Pro. The floodplain boundary was delineated using a 1-meter resolution, bare-earth digital elevation model (2020) obtained from the U.S. Geological Survey.

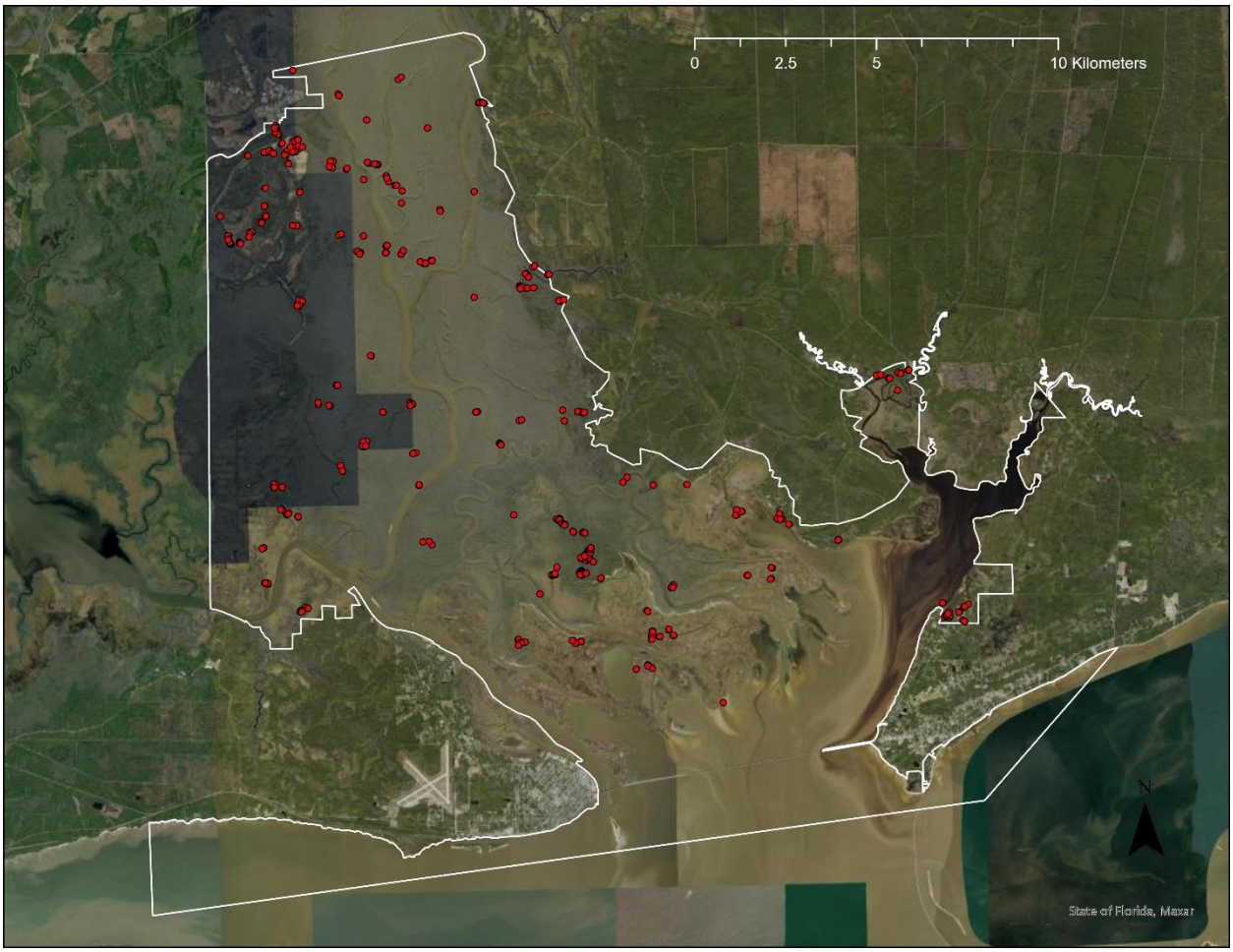

Figure 5. Map showing locations of 600 points that were randomly generated within the AOI using ground truth data. The red dots represent the accuracy points.

2.3 Results

The 4 classified images produced with MLC are presented in Figure 6. The red (cabbage palm) classified pixels seen in the northern edges of the NAIP (Figure 6a) and NDVI (Figure 6b) classified images were primarily mixed forest and existing pine. When the texture band (Figure 6c) was incorporated, the Cabbage Palm class (in red) greatly decreased in the upper river system. The MLC that produced the highest overall accuracy and kappa value was the Texture (Text) classified image (Figure 6c) with an accuracy of 85.7% and a kappa of 0.828 Unfortunately, red pixels along the north-eastern boundary of the texture classified image appear

to have been misclassed as cabbage palm. These areas are located near the previously indicated planted pine (Section 2.4) and is likely pine, considering this area is not wetland. Though this is the class, the Text classified image also produced the highest user accuracy of 88.7% and highest producer accuracy at 94.0% (Table 3).

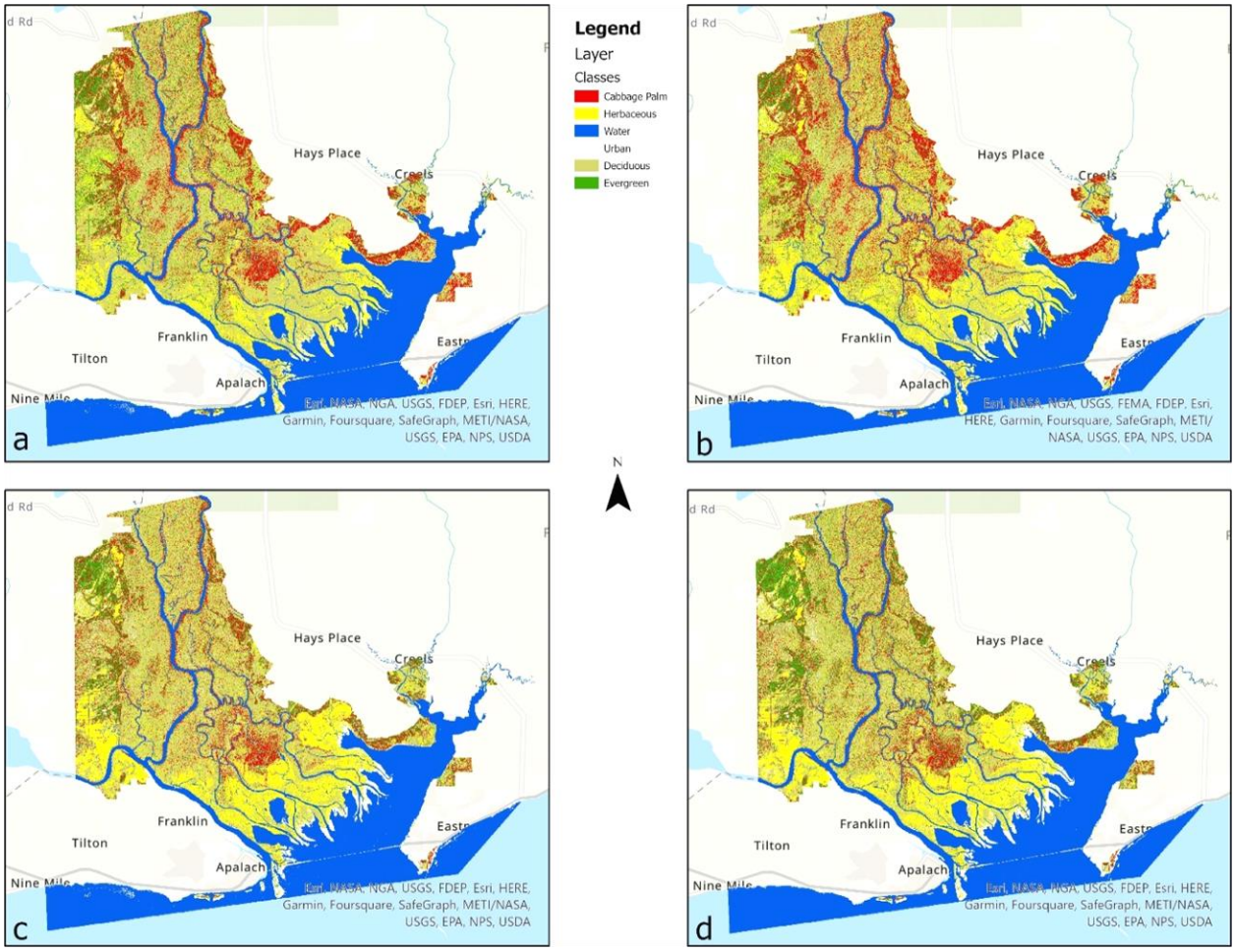

Figure 6. Classified Image Results: Above are the resulting maps of the maximum likelihood classification process.. 6a is the Naip only classified image; 6b is the NDVI and Naip classified image; 6c is the Texture and Naip classidied image; and 6d is the Texture, NDVI, and Naip classified image.

For the NAIP classified image (red, blue, green, and NIR bands) (Figure 6a), there was a 63.8% user accuracy and 88.0% producer accuracy (Table 1) seen in the Cabbage Palm class. A 36.2% commission error was detected, with 29.7% inclusion of pixels from the Evergreen class

(dominated by pine species). The remaining 6.5% commission error (Table 1) was caused by inclusion of ground truth pixels in the Herbaceous, Water, and Deciduous classes, respectively. Due to the high commission error, it is likely that approximately 36% of mapped class cover belongs to another class on the ground. The omission error for the Cabbage Palm class in the NAIP classified image was 12.0% resulting from ground truth cabbage palm pixels being omitted from its correct class (Table 1).

For the NDVI classified image (red, blue, green, NIR, and NDVI bands) (Figure 6b), there was a 56.1% user accuracy and 88.0% producer accuracy for the Cabbage Palm class. The error trend continues in the NDVI classified image where 36.3% of the 43.9% total commission error (Table 2) was due to inclusion of ground truth pixels from the Evergreen class and the remaining commission error caused by the same three classes as in the NAIP classified image. The omission error for this classified image in the Cabbage Palm class was 12.0%, attributed to ground truth cabbage palm pixels being misclassified as the Deciduous, Evergreen, and Herbaceous classes, respectively, when NDVI was incorporated in the classification.

For the texture (Text) classified image (red, green, blue, NIR, and textural bands) (Figure 7c), there was an 88.7% user accuracy and 94.0% producer accuracy for the cabbage palm class (Table 3). The commission error for the Text classified image cabbage palm class was 11.3%, a significant decrease from the previous two classified images. The commission error shows a significant decrease of ground truth pixel inclusion from the Evergreen class (from 29.7% in the NAIP classified image and 36.3% in the NDVI classified image to 5.7% in the Text classified image) (Table 3). The omission error for the Cabbage Palm class in the Text classified image also decreased from the previous two classified images (from 12.0% in the NAIP and NDVI classified images to 6% in the Text classified image). Though a decrease was observed in the

overall omission error, there was a slight increase of ground truth cabbage palm pixels misclassified as Evergreen class (from 3.0% in the NAIP classified image and 2.0% in the NDVI classified image to 5.0% in the Text classified image).

For the N&T classified image (red, green, blue, NIR, NDVI, and textural bands) (Figure 6d), there was an 80.0% user accuracy and 92.0% producer accuracy for the cabbage palm class (Table 4). The commission error for the Cabbage Palm class in the N&T classified image was 20.0% (Table 4). Adding the NDVI band with the texture variance band in the N&T classified image caused an increase in the commission error (Table 4) caused by inclusion the ground truth Evergreen pixels from 5.7% in the Texture classified image to 13.9% in the N&T classified image. An increase in commission error caused by inclusion of ground truth pixels from the Herbaceous class was observed as well, from 1.9% to 3.5%. The overall omission error for the N&T classified image was 8.0%, however, this image had the highest omission error caused by ground truth cabbage palm pixels misclassified as Evergreen class (7.0%) (Table 4).

Confusion with cabbage palm occurred most frequently with the Evergreen class. This trend was seen in all 4 classified image results. The only category that did not impact the commission and omission errors of Cabbage Palm class was Urban (Table 1-4). Considering the user and producer accuracies for all four classified images, along with their respective errors, the Text classified image outperformed the other three classified images and was used for the final product for this study.

Table 1. Confusion matrix of the NAIP only (NAIP) classified image. The accuracy of each class is highlighted in Bold.

NAIP	**Ground Truth (Percent)**			**Overall Accuracy**: 73.3			**Kappa**: 0.68		
Classes	**Cabbage Palm**	**Herbaceous**	**Water**	**Urban**	**Deciduous**	**Evergreen**	**Total Predicted**	**User Accuracy**	**Commission Error**
Cabbage Palm	88.0	6.0	2.0	0.0	1.0	41.0	138	63.8	36.2
Herbaceous	0.0	32.0	0.0	0.0	4.0	1.0	37	86.5	13.5
Water	0.0	0.0	86.0	0.0	0.0	0.0	86	100.0	0.0
Urban	0.0	1.0	0.0	95.0	14.0	0.0	110	86.4	13.6
Deciduous	9.0	61.0	0.0	5.0	81.0	0.0	156	51.9	48.1
Evergreen	3.0	0.0	12.0	0.0	0.0	58.0	73	79.4	20.6
Total Truth	100	100	100	100	100	100	600		
Producer Accuracy	88.0	32.0	86.0	95.0	81.0	58.0			
Omission Error	12.0	68.0	14.0	5.0	19.0	42.0			

Table 2. Confusion matrix for the NAIP and NDVI band (NDVI) classified image. The accuracy of each class is highlighted in Bold.

NDVI	**Ground Truth (Percent)**			**Overall Accuracy**: 71.0			**Kappa**: 0.652		
Classes	**Cabbage Palm**	**Herbaceous**	**Water**	**Urban**	**Deciduous**	**Evergreen**	**Total Predicted**	**User Accuracy**	**Commission Error**
Cabbage Palm	88.0	6.0	5.0	0.0	1.0	57.0	157	56.1	43.9
Herbaceous	1.0	51.0	0.0	3.0	15.0	1.0	71	71.8	28.2
Water	0.0	0.0	83.0	0.0	0.0	0.0	83	100.0	0.0
Urban	0.0	1.0	0.0	95.0	16.0	0.0	112	84.8	15.2
Deciduous	9.0	42.0	0.0	2.0	68.0	1.0	122	55.7	44.3
Evergreen	2.0	0.0	12.0	0.0	0.0	41.0	55	74.5	25.5
Total Truth	100	100	100	100	100	100	600		
Producer Accuracy	88.0	51.0	83.0	95.0	68.0	41.0			
Omission Error	12.0	49.0	17.0	5.0	32.0	59.0			

Table 3. Confusion matrix for the NAIP and Texture band (TEXT) classified image. The accuracy of each class is highlighted in Bold.

Texture	**Ground Truth (Percent)**			**Overall Accuracy**: 85.7			**Kappa**: 0.828		
Classes	**Cabbage Palm**	**Herbaceous**	**Water**	**Urban**	**Deciduous**	**Evergreen**	**Total Predicted**	**User Accuracy**	**Commission Error**
Cabbage Palm	94.0	2.0	3.0	0.0	1.0	6.0	106	88.7	11.3
Herbaceous	0.0	84.0	0.0	3.0	27.0	2.0	116	72.4	27.6
Water	0.0	0.0	90.0	0.0	0.0	0.0	90	100.0	0.0
Urban	0.0	1.0	0.0	96.0	12.0	0.0	109	88.1	11.9
Deciduous	1.0	11.0	0.0	1.0	59.0	1.0	73	80.8	19.2
Evergreen	5.0	2.0	7.0	0.0	1.0	91.0	106	85.9	14.2
Total Truth	100	100	100	100	100	100	600		
Producer Accuracy	94.0	84.0	90.0	96.0	59.0	91.0			
Omission Error	6.0	16.0	10.0	4.0	41.0	9.0			

Table 4. Confusion matrix for the NAIP, NDVI band, and Texture band (N&T) classified image. The accuracy of each class is highlighted in Bold.

NDVI & Texture	**Ground Truth (Percent)**			**Overall Accuracy**: 82.2			**Kappa**: 0.786		
Classes	**Cabbage Palm**	**Herbaceous**	**Water**	**Urban**	**Deciduous**	**Evergreen**	**Total Predicted**	**User Accuracy**	**Commission Error**
Cabbage Palm	92.0	4.0	2.0	0.0	1.0	16.0	115	80.0	20.0
Herbaceous	0.0	81.0	0.0	3.0	26.0	3.0	113	71.7	28.3
Water	0.0	0.0	85.0	0.0	0.0	0.0	85	100.0	0.0
Urban	0.0	0.0	0.0	96.0	14.0	0.0	110	87.3	12.7
Deciduous	1.0	14.0	0.0	1.0	59.0	1.0	76	77.6	22.4
Evergreen	7.0	1.0	13.0	0.0	0.0	80.0	101	79.2	20.8
Total Truth	100	100	100	100	100	100	600		
Producer Accuracy	92.0	81.0	85.0	96.0	59.0	80.0			
Omission Error	8.0	19.0	15.0	4.0	41.0	20.0			

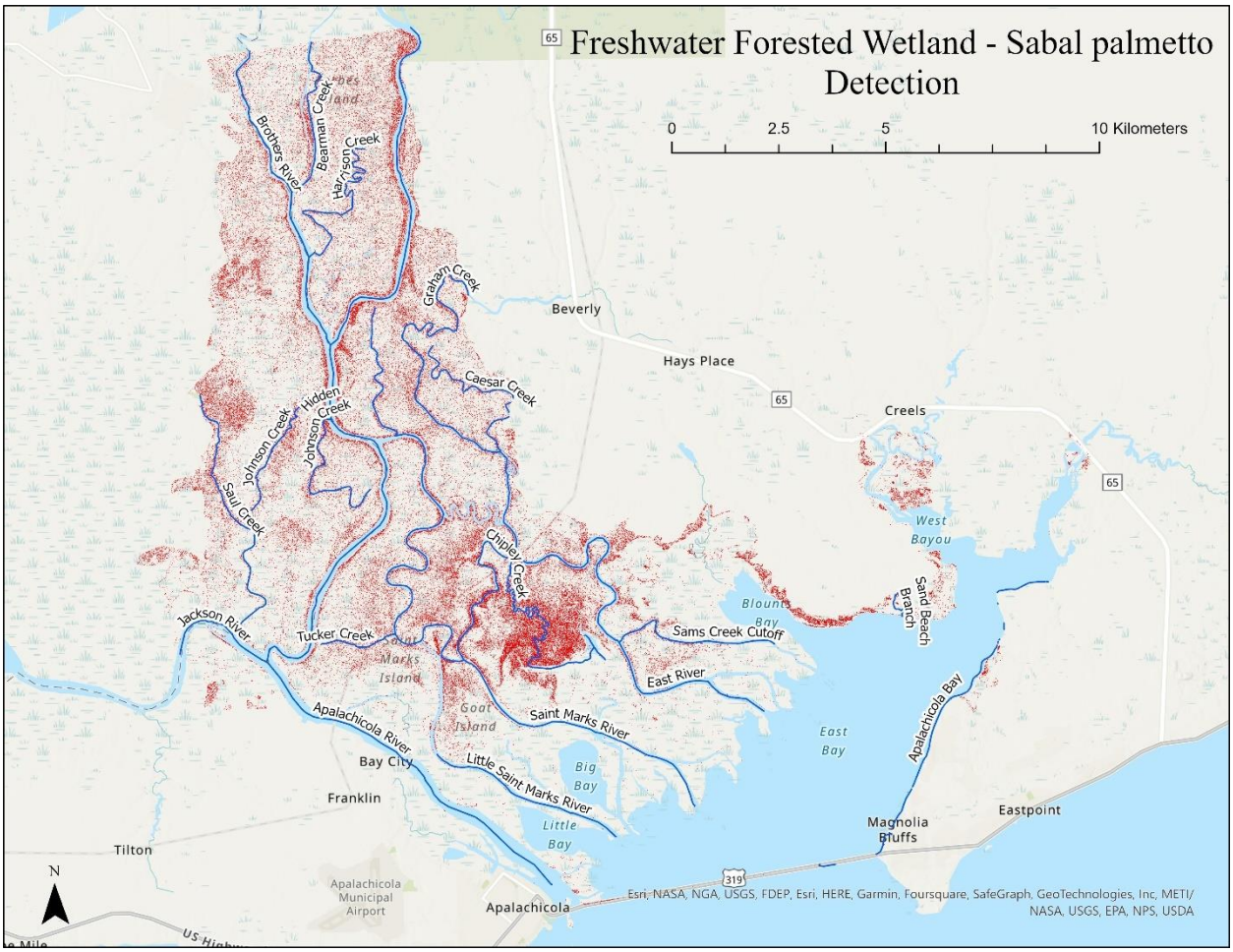

Figure 7. Cabbage Palm class extracted from the Text classified image. The scale of this image is 1:105,000 meters. The area represented in red is the Cabbage Palm class.

2.4 Discussion

The use of the NIR textural variance band had a positive effect on the detection of cabbage palm within a freshwater forested wetland ecosystem. Though cabbage palm detection does not allow for a discrete tidal/nontidal freshwater forested boundary to be established, dense stands of cabbage palm appear along river edges and a large stand can be seen in the transitional zone directly above the marsh. Of the 27,876.1 ha AOI, a total of 2,279.3 ha of cabbage palm (Figure 6c) was detected within the study area. The revised area (restricted to only the Apalachicola River floodplain) has a total area of 19,303.8 ha (Figure 7). This brought the total

detected cabbage palm area to 1,472.1 ha. In most locations cabbage palm was detected along waterways, moving away from the rivers appears to decrease the concentration of cabbage palm in those areas (0 – 1,886 cabbage palm pixels per hectare). This agrees with the findings of Wade and Langdon (1990), that cabbage palm found in the northern reaches of its natural range (northern Florida and southern Georgia) typically occur in flood plains along major rivers and in periodically flooded lowlands.

Particularly noteworthy, a very dense stand of cabbage palm can be seen between the East and Saint Marks Rivers directly north of marsh wetlands along the bay (Figure 7). This area has a cabbage palm pixel density of between 8,755 to 15,056 pixels per hectare. This aligns with the findings of Williams et al. (1999) that cabbage palm was the only living tree species in the most frequently flooded tidal areas in the Waccasassa Bay State Preserve, Florida. Williams et al. (1999) also found an "anomalously" high density of cabbage palm along with *Cladium jamaicense* (a marsh species characteristic of freshwater or brackish marsh), though the conditions allowing this phenomenon were uncertain. This area is near the TFFW and tidal marsh boundary (close to the bay) and would likely experience routine salinity intrusion. This aligns with a study by Celik et al. (2020) that found increased salinity along the lower reaches of the St. Marks River (0.02ppt – 12.7ppt) (west of the dense cabbage palm stand – Figure 7) and the East River (0.02ppt – 10.8ppt) (east of the dense cabbage palm stand – Figure 7). A relatively small tidal creek (Chipley Creek) with no direct connection with the East River or the St. Marks River flows directly through this large stand of cabbage palm (Figure 7) and therefore is unlikely to get the same freshwater flows that many other TFFWs experience along these rivers. Unlike TFFWs seen elsewhere (Anderson and Lockaby, 2011), this appears to be forested area within the lower Apalachicola River system where cabbage palm is the dominant canopy species.

Chipley Creek could play a role in hydrology allowing the cabbage palm to flourish in this area, but further investigation is required. Another large stand dominated by cabbage palm (1.886-3,772 cabbage palm pixels per hectare) was detected near Sand Beach Branch along East Bay and further from the river.

Cabbage palm was detected along most of the creeks and rivers within the study area with Apalachicola River appearing to have the most cabbage palm along its reach from Tucker Creek upward to the edge of the river at the northern AOI boundary (Figure 7). The densest section of cabbage palm detected along the Apalachicola River edge can be seen just above Hidden Johnson Creek, continuing north to the river's edge at the northern AOI boundary (Figure 7). The density for this section of cabbage palm pixels is between 1,886 and 3,772 per hectare. Cabbage palm, though not as dense, was also detected (1,886 – 3,772 cabbage palm pixels per hectare) along Hidden Johnson Creek, Johnson Creek, and Saul Creek to the west of the Apalachicola River, and Saint Marks River, East River, and Sams Creek Cutoff to the east with a cabbage palm pixel density between 1,886 – 5,657 per hectare. Relatively dense cabbage palm (3,772 – 5,657 pixels per hectare) can also be seen between Apalachicola River and northern reach of the Saint Marks River. This pattern of cabbage palm detection along river edges throughout the study area could be related to the natural levees that form on the river's edge due to sediment deposition during flood events (Mitsch and Gosselink, 2015). These natural levees are often the highest elevation within a floodplain (Mitsch and Gosselink, 2015) and create raised areas that allow for seedlings to take root out of the direct waterline while still experiencing periodic flooding from the river. Cabbage palm seedlings have been observed in areas with flooded conditions for up to 13 weeks (Williams et al., 1999) with adult cabbage palms preference for sandy soils on periodically flooded lowlands (Wade and Langdon, 1990).

Seedlings have also been observed to have improved performance (photosynthetic rates) in plants that experience continuous flooding with freshwater, though tidal flooding was correlated with seedling mortality (Williams, 1996). Cabbage palm also appears frequently along the convex sides of meandering rivers (Saint Marks River, Chipley Creek, and Apalachicola River in Figure 7). This could be associated with the formation of point bars within convex curves of rivers from sediment deposition at or below the bankfull river stage (Mitsch and Gosselink, 2015) and are often predominately sandy soils.

Of all four classified images, the Text classified image had the highest overall accuracy (85.7%) with a kappa value of 0.828, as well as the highest user (88.7%) and producer (94.0%) accuracies for the Cabbage Palm class (Table 3). Congruent with the findings from Xie et al. (2019), the MLC accuracy did improve with the addition of the texture band versus just the image bands (red, blue, green, and NIR) in the classification of forested land cover for the leaf-off season. Studies have shown to achieve similar accuracies and kappa values as those found in this study. Using the MLC for forest cover in 1990, 2013, and 2017 in Goaso Forest District, Ghana, Lossou et al. (2019) achieved overall accuracies between 90.3% and 95.0% and kappa values between 0.878 and 0.937. Rodriguez-Galiano et al. (2012) performed classifications on 14 different land cover types, one of which was conifers in Granada Province, Spain. Using the MLC, the overall accuracy achieve was 84% with a kappa value of 0.84, while their conifers class achieved a user accuracy of 81.0% and a producer accuracy of 78.0% (Rodriguez-Galiano et al., 2012).

Although incorporating the textural band did improve the accuracy, Ferreira et al. (2019) found that textural analysis using a panchromatic band (0.3m spatial resolution) yields better results. For future studies of this area, an image data source with a higher spatial resolution

(<1m) should be considered for improved crown structure separation. Still, all resulting classified images from this study yielded overall accuracies between 71.0% - 85.7%. The final product (Figure 7) of this study shows cabbage palm detected through the study area, with concentrations at the bottom edge of the forested area between Saint Marks and East River as well as along much of the rivers' edge. This suggests that there may be more variables not considered in this study that impact the distribution of cabbage palm within the Apalachicola area. In observations from Anderson and Lockaby (2011), non-tidal forested wetlands showed larger trees than the tidal forested wetlands, however, tree density was higher in the tidal systems than in the non-tidal (Anderson & Lockaby, 2011; Anderson, et. al 2013). If this observation is a characteristic of tidal versus non-tidal forested wetlands, canopy height (e.g., derived from lidar data) could aid in identifying the shift from tidal to non-tidal in the forested wetlands of Apalachicola at a finer scale in future studies.

2.5 Conclusion

Several areas of cabbage palm (a previously identified TFFW indicator species) were detected along the lower Apalachicola River system. Concentration of cabbage palm density along the lower reach of the floodplain that is not along the main stem of the Apalachicola River suggests that increased freshwater input from the larger river (Apalachicola River versus St. Marks and East River) allows for more non-tidal forested species to persist closer to the bay. However, as we move east, we see a dense cluster of cabbage palm at the center of the lower floodplain before a discrete transition to herbaceous vegetation. The Texture band proved efficient in the detection of cabbage palm species with the use of NAIP high spatial resolution imagery (from 63.8% to 88.7% user accuracy), however, inclusion of the NDVI band had a negative impact on cabbage palm detection (from 88.7% to 80.0% user accuracy).

Recommendations for future studies to improve the accuracy of tidal/non-tidal composition include: 1) limiting the study area strictly to the Apalachicola River floodplain to limit confusion with pine and 2) incorporate canopy height information, such as high-resolution canopy height models generated from lidar data.

References

Anderson, C. J., & Lockaby, B. G. (2011). Forested Wetland Communities as Indicators of Tidal Influence along the Apalachicola River, Florida, USA. *Wetlands*(31), 859-906. doi:https://doi.org/10.1007/s13157-011-0204-5

Anderson, C. J., Lockaby, B. G., & Click, N. (2013). Changes in Wetland Forest Structure, Basal Growth, and Composition across a Tidal Gradient. *The American Midland Naturalist, 170*(1), 1-13. doi:10.1674/0003-0031-170.1.1

Anys, H., A. Bannari, D. C. He, and D. Morin. "Texture analysis for the mapping of urban areas using airborne MEIS-II images." *Proceedings of the First International Airborne Remote Sensing Conference and Exhibition* 3 (1994): 231-245.

Brown, K.E. (1973). Ecological life history and geographical distribution of the cabbage palm, *Sabal palmetto.* Ph.D. Dissertation, University of Florida, Gainesville, Florida.

Cecilia, D. l., Toffolon, M., Woodcock, C. E., & Fagherazzi, S. (2016). Interactions between river stage and wetland vegetation detected with a Seasonality Index derived from LANDSAT images in the Apalachicola delta, Florida. *Advances in Water Resources, 86*, 10-23. doi:10.1016/j.advwatres.2015.12.019

Celik, S., Anderson, C. J., Kalin, L., & Rezaeianzadeh, M. (2020). Long-term Salinity, Hydrology, and Forested Wetlands Along a Tidal Freshwater Gradient. *Estuaries and Coasts*. doi:10.1007/s12237-021-00911-8

Chen, S., Huang, W., Wang, H., & Li, D. (2009). Remote sensing assessment of sediment re-suspension during Hurricane Frances in Apalachicola Bay, USA. *Remote Sensing of Environment, 113*(12), 2670-2681. doi:10.1016/j.rse.2009.08.005

DeSantis, L. R., Bhotika, S., Williams, K., & Putz, F. E. (2007). Sea-level rise and drought interactions accelerate forest decline on the Gulf Coast of Florida, USA. *Global Change Biology*, 13(11), 2349-2360. doi:10.1111/j.1365-2486.2007.01440.x

Doyle, T. W., O'Neil, C. P., Melder, M. P., From, A. S., & Plata, M. M. (2007). Tidal Freshwater Swamps of the Southeastern United States: Effects of Land Use, Hurricanes, Sea-level Rise, and Climate Change. *Ecology of Tidal Freshwater Forested Wetlands of the Southeastern United States*. doi:10.1007/978-1-4020-5095-4_1

ESRI. (n.d.). *About arcgis pro*. About ArcGIS Pro-ArcGIS Pro | Documentation. Retrieved October 3, 2022, from https://pro.arcgis.com/en/pro-app/2.8/get-started/get-started.htm

Ferreira, M. P., Wagner, F. H., Aragao, L. E.O.C., Shimabukuro, Y. E., de Souza Filho, C. R. (2019). Tree species classification in tropical forests using visible to shortwave infrared WorldView-3 images and texture analysis. *ISPRS Journal of Photogrammatry and Remote Sensing*, 149, 119-131. doi: 10.1016/j.isprsjprs.2019.01.019

Hall-Beyer, M. *The GLCM tutorial home page*. http://www.fp.ucalgary.ca/mhallbey/tutorial.htm. Updated February 2007. Accessed March 2016.

Haralick, R., Shanmugan, K., and Dinstein, I. "Textural Features for Image Classification." *IEEE Transactions on Systems, Man, and Cybernetics* 3, no. 6 (1973): 610-621.

Jeter, G.W. and Carter, G.A. (2016). Habitat change on Horn Island, Mississippi, 1940-2010, determined from textural features in panchromatic vertical aerial imagery. *Geocarto International,* 31(9), 985-994.

L3Harris Geospatial Solutions, Inc. (n.d.). *Software & technology: ENVI*. L3Harris Geospatial. Retrieved October 3, 2022, from https://www.l3harrisgeospatial.com/Software-Technology/ENVI

Liang, F., Zhang, X., Li, H., Yu, H., Lin, Q., Jiang, M., & Zhang, J. (2022). Land Use Classification Based on Maximum Likelihood Method. *Advances in Intelligent Data Analysis and Applications*, 133-139. doi:10.1007/978-981-16-5036-9_15

Liu, X., Conner, W. H., Song, B., & Jayakaran, A. D. (2017, April). Forest composition and growth in a freshwater forested wetland community across a salinity gradient in South Carolina, USA. *Forest Ecology and Management, 389,* 211-219.

Livingston, R. J. (1984). *The ecology of the Apalachicola Bay system: an estuarine profile.* Washington, D.C.: U.S. Department of the Interior.

Lossou, E., Owusu-Prempeh, N., and Agyemang, G. (2019). Monitoring Land Cover changes in the tropical high forests using multi-temporal remote sensing and spatial analyses techniques. *Remote Sensing Applications: Society and Environment*, 16, 100264. doi: 10.1016/j.rsase.2019.100264

MacFaden, S.W., O'Neil-Dunne, J.P.M, Royar, A.R., Lu, J.W.T, and Rundle, A.G. (2012). High-resolution tree canopy mapping for New York City using LiDAR and object-based image analysis. *Journal of Applied Remote Sensing,* 6(1). doi: 10.1117/1.JRS.6.063567

Masek, J.G, Vermote, E.F., saleous, N.E., Wolfe, R., Hall, F.G., Huemmrich, K.F., Gao, F., Kulter, J., and Lim, T. (2006). A Landsat surface reflectance dataset for North America, 1990-2000. *IEEE Geoscience and Remote Sensing Letters*, 3(1), 68-72. doi: 10.1109/LGRS.2005.857030

Mitsch, W. J., & Gosselink, J. G. (2015). *Wetlands* (Fifth ed.). Hoboken, New Jersey: John Wiley & Sons, Inc.

Rodriguez-Galiano, V.F, Chica-Olmo, M., Abarca-Hernandex, F., Atkinson, P.M., and Jeganathan, C. (2012). Random Forest Classification of Mediterranean land cover using multi-seasonal imagery and multi-seasonal texture. *Remote Sensing of Environment,* 121, 93-107. doi: 10.1016/j.rse.2011.12.003

Paine, D. P. (1981). Aerial Photography and Image interpretation for Resource Management.

John Wiley & Sons, Inc.

Patel, D., and T. J. Stonham. "Texture Image Classification and Segmentation using RANK-Order Clustering." *11th IAPR International Conference on Pattern Recognition* (1992), pp. 92-95.

United States Environmental Protection Agency. (2013). *Wetlands - Status and Trends*. Retrieved from EPA: https://archive.epa.gov/water/archive/web/html/vital_status.html

United States Environmental Protection Agency. (2021, September 3). *Wetlands Protection and Restoration*. Retrieved from EPA: https://www.epa.gov/wetlands

U.S. Fish & Wildlife Service. (2021). NWI Code Definitions Table. National Wetlands Inventory | U.S. Fish & Wildlife Service. Retrieved April 30, 2022, from https://www.fws.gov/program/national-wetlands-inventory

U.S. Fish & Wildlife Service. (2022). National Wetlands Inventory. *National Wetlands Inventory | U.S. Fish & Wildlife Service*. Retrieved April 30, 2022, from https://www.fws.gov/program/national-wetlands-inventory

Vermote, E., Justice, C., Claverie, M., & Franch, B. (2016). Preliminary analysis of the performance of the Landsat 8/OLI land surface reflectance product. *Remote Sensing of Environment*, 185, 46-56

Wade, D. D. and Gordon Langdon (1990). *Sabal Palmetto* (Walt.). Lodd, Ex JA & JH Schult. cabbage palmetto. Silvics of North America, 2, 762-767.

Waldron, B., Claire, M., Carter. G.A., & Biber. P.D. (2021) Using Aerial Imagery to Determine the Effects of Sea-Level Rise on Fluvial Marsh at the Mouth of the Pascagoula River (Mississippi, USA). *Journal of Coastal Research*, 37(2), 389-407. doi: 10.2112/JCOASTRES-D-20-00037.1

Wang, H., Dai, Z., Terttin, C. C., Krauss, K. W., Noe, G. B., Burton, A. J., . . . Ward, E. J. (2022). Modeling impacts of drought-induced salinity intrusion on carbon dynamics in tidal freshwater forested wetlands. *Ecological Applications*. doi:10.1002/eap.2700

Ward, G. M., Harris, P. M., & Ward, A. K. (2005). Gulf Coast Rivers of the Southeastern United States. In A. C. Benke, & C. E. Cushing (Eds.), *Rivers of North America*, 125-178. USA: Elsevier Academic Press.

Warner, T. "Kernel-based Texture in Remote Sensing Image Classification." *Geography Compass* 5/10 (2011): 781-798. doi: 10.1111/j.1749-8198.2011.00451.x

Williams, K., Ewel, K. C., Stumpf, R. P., Putz, F. E., and Workman, T. W. (1999). Sea-Level Rise and Coastal Forest Retreat on the west coast of Florida, USA. *Ecology*, 80(6), 2045-2063.

Williams, P. K. (1996). Effects of salinity and flooding on seedlings of cabbage palm (Sabal palmetto). *Oecologia*, 105, 428-434.

White Jr., E. E., Ury, E. A., Berhardt, E. S., & Yang, X. (2022). Climate Change Driving Widespread Loss of Coastal Forested Wetlands Throughout the North American Coastal Plain. *Ecosystems, 25*, 812-827.

Xie, Z., Chen, Y., Lu, D., Li, G., Chen, E. (2019). Classification of Land Cover, Forest, and Tree Species Classes with ZiYuan-3 Multispectral and Stereo Data. *Remote Sensing*, 11, 164. doi: 10.3390/rs11020164

Zona, S. (1990). A monograph of Sabal (Arecaceae: Curyphoidaea). *Aliso: A Journal of Systematic and Floristic Botany*, 12(4), 583-666. doi: 10.5642/aliso.19901204.02

Chapter 3: Assessing the spatial extent of *Juncus roemerianus* in Apalachicola, Florida using Landsat imagery

Abstract

Tidal marsh wetlands are an important natural resource that are affected by salinity which can vary based on multiple factors such as changing river flows, hurricanes and tropical storms, droughts, and sea level rise. The use of satellite imagery to bridge the gap in knowledge of marsh landscapes is at the forefront of environmental modeling and aid in providing information to land managers about past and future changes. The aim of this study was to map and quantify the changes in the marsh communities of the lower Apalachicola River, Florida, USA from 2008 to 2014 to 2022 using Landsat imagery. Given the fluctuation of average annual river flow discharge from Apalachicola River (ranging from 9,677 to 35,120 cubic feet per second between 2000 and 2022), understanding how marsh communities shift over time could provide insight to possible impacts in the future. Maximum Likelihood classification was utilized in this study to map the extent of black needlerush (*Juncus roemerianus*, henceforth *Juncus)*, a common and relatively salt tolerant marsh species within the lower river deltaic region. The resulting classifications from this study produced overall accuracies above 90% using Landsat imagery. The spatial extent of *J. roemerianus* was evaluated during the three periods: 2008, 2014 and 2022. Most years leading up to 2008 and from 2008-2014 were characterized by lower than average annual river flows caused by regional drought. The years from 2014-2022 were characterized by above average rivers flow. Change detection analyses from 2008 to 2014 found a 596.3 ha increase and a 144.7 ha decrease in the *Juncus* marsh extent, while change between 2014 to 2022 found a 157.8 ha increase and a 371.4 ha decrease in the *Juncus* marsh. These results indicate that relative river flow and its control of the lower river salinity may play a role

in changing marsh composition. Outcomes from this work will facilitate continued monitoring of the Apalachicola marshes as well as promote informed management practices. Utilizing this approach for continued monitoring could aid in promoting better understanding of the effects of drought on these wetland communities.

Key Words: Coastal wetlands, Apalachicola, Tidal marshes, *Juncus roemerianus*, Remote sensing

3.1 Introduction

It is important to document possible marsh transitions related to environmental change. Understanding impacts to marsh ecosystems that provide many important services, including but not limited to, water purification, storm surge buffering, and fish nursery habitat is needed to better manage these natural resources (NOAA Fisheries, 2022). Tidal marshes are often typified by a dominant vascular plant species, which can change depending on the region (Stout, 1984). Though there are typical patterns seen in the distribution across a marsh landscape, competition between marsh species can also shape the distribution of marsh communities, along with outside environmental factors, making it difficult to predict changes to marsh composition in response to land management practices (Townend et al., 2011). Due to shifts in conditions across a tidal gradient (ranging from freshwater to intermediate salinity) in marsh systems, distinct zonation of near-monocultural patches of different species can occur (Hackney et al., 1996). For example, for salt marshes in the southeast United States, species such as *Spartina alterniflora* are found predominately in tidal marshes but other species (such as *Juncus roemerianus*, henceforth *Juncus*) may be more common where freshwater influence increases (Touchette et al., 2009). Zonation of tidal marsh communities commonly occur in river deltas where salinities are influenced by the freshwater flows coming from the river. In these situations, tidal marshes are more brackish but species assemblages are still responding to gradients of salinity (Mitsch & Gosselink, 2015). This pattern can be seen in the lower Apalachicola River in west Florida, with *Juncus* as one of the dominant halophytic marsh species but often transitioning to saw grass (*Cladium jamaicense*) and other species typical of more oligohaline conditions (Harper, 1911; Field, et al., 1991; Edmiston, 2008). *Juncus* spreads via extensive rhizome growth, allowing for a single individual to cover large portions of the marsh surface (Stout, 1984) and is known to be

stable along the coast, with patch stability resulting from the wide tolerance of hydroperiod and salinity (Brinson & Christian, 1999).

Although there is wide interest in mapping tidal marshes, few studies have been conducted to evaluate shifts in *Juncus* using remote sensing techniques. In a study by Ramsey III and Rangoonwala (2004), the optical properties of *Juncus* were compared with other marsh vegetation types within the St. Marks National Wildlife Refuge (northeast U.S. Gulf of Mexico) and they found the narrow cylindrical leaves of this species had a unique visible leaf reflectance when compared. Another study by Ramsey III et al. (2002) successfully utilized the Landsat Thematic Mapper along with the Normalized Difference Vegetation Index (NDVI) to monitor the recovery of *Juncus* marsh following burns. These studies aid in building a foundation for remote sensing of marsh species (specifically *Juncus)* but have not applied this approach for a time series assessment of marsh community types. Due to its unique spectral profile and the fact that *Juncus* has been observed to be abundant in the saltier marshes of the Apalachicola River and Bay region (Edmiston, 2008; Livingston, 1984), it was selected as a suitable indicator species for gaging salinity shifts in this study.

Mapping fluctuations in marsh species cover over time can reveal patterns related to changing environmental conditions, which may be useful to predict potentially more permanent shifts in community composition. Sea level rise (SLR), increased tropical storm activity and changes in river flows may alter tidal river marsh salinities and shift marsh plant assemblages. The use of traditional field survey methods to capture this variation in vegetation community distribution over a range of spatial and temporal scales is limited due to labor cost and time constraints. The availability of satellite remotely sensed data allows for the mapping of vegetation for a comprehensive assessment of spatial properties and relationships between and

within diverse marsh communities (Townend et al., 2011). Vegetation is a common indicator of specific hydrological and chemical characteristics of a system, such as a tidal marsh (Hackney et al., 1996), thus providing a means of determining important changes and their extent within the ecosystem (Crain et al., 2004). Satellite imagery and imagery-derived vegetation indices have been used in previous studies to monitor marsh vegetation communities and to improve overall performance and accuracy of environmental models (Correll et al., 2018; Campbell & Wang, 2020; Zhang et al., 2020; Waldron et al., 2021; Yang et al., 2022). One study found that the NDVI was the best-performing vegetation index used in modeling salt marsh extent, achieving between 90% and 95% producer's accuracy for the salt marsh (Lopes et al., 2020). A study by Campbell and Wang (2020) utilized several spectral indices in the monitoring of salt marshes along the east coast of the USA along the mid-Atlantic these indices included: Wide Dynamic Range Vegetation Index (WDRVI), Soil Adjusted Vegetation Index (SAVI), Normalized Difference Red Green, Normalized Difference Green Blue, Normalized Difference Shortwave Infrared 2 (SWIR2) Red, Normalized Difference SWIR2 NIR, and Normalized Difference Water Index (NDWI). These indices aided in a land cover change assessment of salt marshes dominated by *Spartina alterniflora*, *Juncus gerardii*, *Spartina patens*, *Distichlis spicata*, and *Juncus roemerianus* (Campbell & Wang, 2020).

Though extensive field work has historically been conducted in the Apalachicola estuary, very little detail has been recorded in the freshwater and brackish marsh communities in the lower river and upper bay region (Edmiston, 2008). Using tidal marshes in the lower Apalachicola River, the primary goal of this study was to identify shifts in the marsh vegetation communities over the last two decades. Over that time, there has been significant shifts in annual river flows to Apalachicola Bay that have likely affected tidal marsh communities in the river

delta. Further, there has been increasing sea level rise detected in the bay that may also influence marsh salinity and community shifts. Specifically, this work served to apply Landsat imagery for image classification of *Juncus* (the dominant species occupying the more saline portions of the lower river) to identify potential marsh community shifts along the lower Apalachicola River as it relates to annual shifts in river flow. This river system connects with the Apalachicola Bay allowing tidal marshes to occur across a gradient of salinities affected by both the bay and the river. Studying patterns of cover within transitional plant communities (a mixture of freshwater and brackish marsh species) will provide beneficial information to resource managers as they address environmental risks and future changes along the Apalachicola River related to river flow, tropical storms, and sea level rise (SLR). For this study, shifts in the extent of *Juncus* marsh cover were expected, specifically, increases in *Juncus* following drought years and decrease following wetter years with above-average river flows.

3.2 Methodology

3.2.1 Study Area

The study area boundary (or area of interest – AOI) for this study was delineated using the Emergent Vegetation and Woody Wetland classes from the National Wetland Inventory (U.S. Fish & Wildlife Service, 2022) as a reference for existing marsh extent. This product provides information and geospatial products on existing wetland extent and status of national wetlands and deep-water habitats in the United States. Emergent Vegetation and Woody Wetland classes were included due to the mixture of freshwater forested wetland and marsh wetland dynamic community near the river mouth.

The lower Apalachicola River and Apalachicola Bay is in the panhandle of Florida, USA (Figure 1) and is a large coastal outlet for three major rivers in the Southeastern United States: the Apalachicola, Chattahoochee, and Flint Rivers (Livingston, 1984). Understanding and managing this region are crucial because of historically important fisheries in the bay and the variety of stressors that can impact the stability of its ecosystems. Within the area, there is approximately 7,865 hectares (ha) of tidal marshes extent and 3,181 ha of submerges aquatic vegetation (Edmiston, 2008). In 2008, 703 ha of marsh land is accounted for in the Apalachicola Bay while 4,604 ha of marsh land is accounted for in the East Bay (Edmiston, 2008), totaling 5,307 ha of marsh cover within the study area. Marshes found in the estuary include freshwater, brackish, and salt marsh, which cover approximately 17% of the total aquatic area (Edmiston, 2008).

Freshwater marshes in this area are predominantly comprised of bullrushes (*Scirpus* spp.), cattails (*Typha* spp.), and sawgrass (*Cladium jamaicense*) marsh species while the more brackish marshes contain more black needlerush (*Juncus roemerianus)* and cordgrasses (*Spartina* spp.) (Edmiston, 2008; Livingston, 1984; Leitman, 1983). Brackish and salt marsh systems can also be found on St. Vincent Island (southwest of the study area) where the dominant wetland vegetation species are black needlerush, smooth cordgrass, and salt grass (*Distichlis spicata*) (Edmiston, 2008). Sawgrass-dominant marshes have been observed in areas with a higher influence of river flow, typically associated with lower salinity, whereas black needlerush has been observed in marshes within the tidal areas typically associated with higher salinity (Livingston, 1984).

Salinity within the Apalachicola estuary ranges from 0 parts per thousand (ppt) to 33 ppt moving north to south along the Apalachicola River into the bay (Edmiston, 2008). Generally,

salinity observations have also been seen to increase moving west to east along the bay (Edmiston, 2008). Some of the dominant drivers of the wetland structure and salinity gradient seen in the Apalachicola estuary are river flow, physical geography, and seasonal changes of nutrients (Livingston, 1984). The lower reach of the Apalachicola River has been recorded reaching salinities around 0.5 ppt (Livingston, 1984). The average daily salinity levels of the lower St. Marks and East Rivers that feed into the bay-edge marshes is between 0.6 ppt and 0.3 ppt, respectively, but can exceed 10ppt when river flows become low (Celik, et al., 2020). This salinity gradient results in varied transitional areas between freshwater and brackish conditions with the Apalachicola marshes. Because of the limited work performed in this area to assess the "salt wedge" in the lower Apalachicola River systems, its true extent is uncertain (Edmiston, 2008). This study provides an overview of the marsh in this area while also demonstrating a framework for modeling the extent of *Juncus* to monitor change over time.

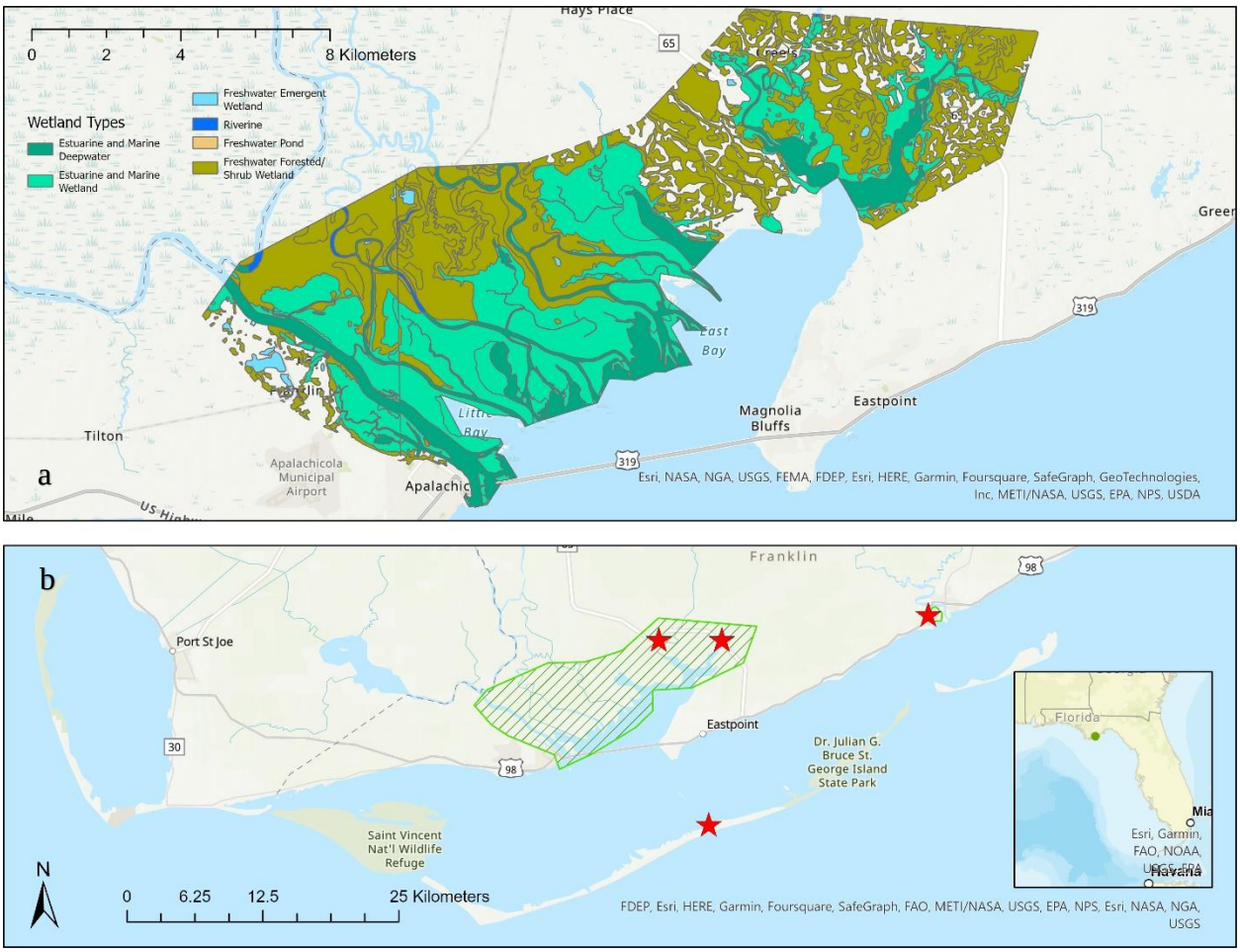

Figure 1. Map of the Apalachicola Marsh Study area (a). This map represents the point location data collected in May 2022 and two areas with known Juncus stands (b). The green represents the study area, the red represents the data points collected using ArcGIS Survey123 (ESRI, 2022).

3.2.2 River and Remote Sensing Data

3.2.2.1 Apalachicola River Flow

Figure 2. Above are images of Juncus marsh. The image to the left is an image of a Juncus marsh within the Apalachicola study area. The image on the right is an aerial view of Juncus marsh from Google Earth (n.d) from https://earth.google.com/web/@29.82366752,-84.90250674,0.82096577a,219.84071198d,35y,0h,0t,0r .

Salinity regimes in the lower Apalachicola River, including tidal marshes, is highly dependent on river flows that vary seasonally and annually. To evaluate the effect of river flow on marsh community dynamics, three separate years were selected at eight-year intervals: 2008, 2014 and 2022. Figure 3 represents the average discharge of a monitoring gage for Apalachicola River near Sumatra, Florida (gage seen in Figure 1). The three red lines seen (Figure 3) are for the years 2008, 2014, and 2022, and the gray dashed line is the average annual discharge from 2000 to 2021 (the last recorded annual discharge). The gray dotted line is the average monthly discharge from July to December for each year, 2000 and 2021. It is during these months when river flow is typically the lowest. In the years approaching 2008, a steep drop in annual average discharge is seen (2006 to 2008). After 2008, there was a spike in 2010 in streamflow discharge followed by another drought from the end of 2010 to 2012. The year 2013 marks a gradual increase in streamflow discharge. These transitional periods in streamflow discharge are important to understanding lower river salinities and the composition of the marsh with reference to freshwater input. Given 2008 was a drought year, 2014 was a year of increased streamflow but

only a slight increase above the average, and 2022 follows a gradual, consistent increase in streamflow, this allows us to see an overview of the marsh composition in three different stages of freshwater flow.

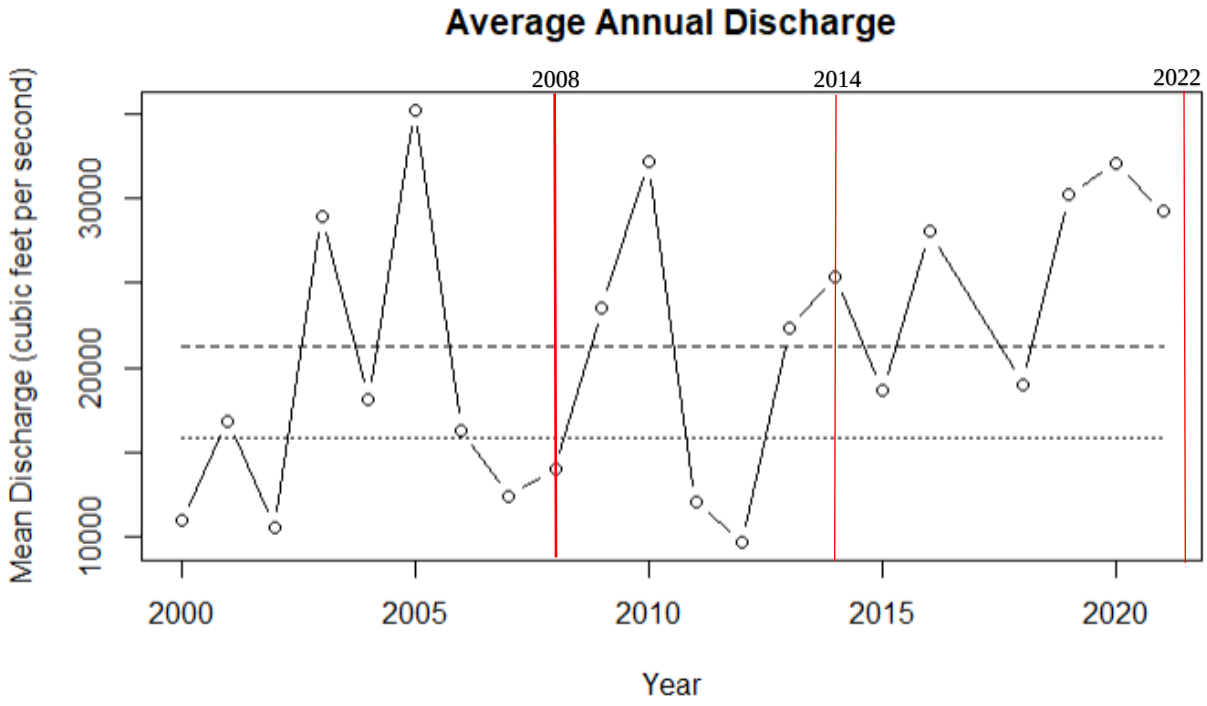

Figure 3. Average annual discharge from the Apalachicola River into the Apalachicola Bay. The thick dashed line represents the average discharge over the timeframe and the dotted line represents the average monthly discharge for fall and winter. The monitoring station is located near Sumatra, Florida (site number: 02359170). This data was retrieved from the USGS StreamStats: https://waterdata.usgs.gov/nwis/rt.

3.2.2.2 Remote Sensing Data

Juncus roemerianus occurs in saline, brackish, and intermediate coastal marshes and comprises one of the largest vegetation zones in the northeastern region of the Gulf coast (Stout, 1984). Given the spatial resolution of Landsat (30-meter), large patches of homogeneous marsh were required for sample sites to train the image classifier used in this study and the zonation of

the *Juncus* in the Apalachicola marsh (described in Section 1) provides an adequate aerial extent discernable from Landsat imagery.

The coordinate system used for all data was WGS 1984 UTM Zone 16N. Three Landsat Collection 2 Level 2 images were downloaded from USGS Earth Explorer from 2008 to 2022. Images were selected during the summer growing season (May 1 to July 1). Landsat was chosen for its continuous archive dating back to the 1970s and the previous success in image classification reported in other studies (Baker et al., 2006; Campbell & Wang, 2020; Lopes, et al., 2020; Zhang, et al., 2020; Yang, et al., 2022). The image from 2008 was acquired by Landsat 5 Thematic Mapper (TM). The images for 2014 and 2022 came from the Landsat 8 Operational Land Imager (OLI) and Thermal Infrared Sensor (TIRS) satellite. All Landsat products have a 30-meter spatial resolution with a 16-day temporal resolution for imaging. Bands for the Landsat missions were revised between satellites due to improvements in technology, resulting in adjustments to the band number and information available per satellite. The bands downloaded and used to create the spectral indices and perform image classification, are listed in Table 1. The study area is located in a single Landsat scene at path 019, row 039. Products containing over 30% land cloud cover were filtered out of the target season (May – July) for each year, then inspected for cloud coverage within the study area. One study found pixel-based image classifications of coastal wetlands can be restricted due to cloud cover and cloud shadows within the image frame as well as the lack of "good-quality" observations of phenological phases given the 16-day cycle (Zhang et al., 2020). Images for the target season before 2008 were omitted due to cloud cover within the study area and lack of validation data (NAIP or survey points collected in the field in 2022). The image from May 5, 2008 had 17% land cloud cover. The image from

May 22, 2014 had 0.28% land cloud cover. The image from May 12, 2022 had 0.17% land cloud cover.

Table 1. Spectral resolution for each of the Landsat Satellites and their corresponding bands (U.S. Department of the Interior, 2022).

Band Name	**Landsat 4-5 Band Ranges**	**Landsat 8-9 Band Ranges**
Blue	0.45-0.52	0.45-0.51
Green	0.52-0.60	0.53-0.59
Red	0.63-0.69	0.64-0.67
Near-InfraRed (NIR)	0.77-0.90	0.85-0.88
Shortwave-InfraRed (SWIR)	1.55-1.75	1.57-1.65

An online GIS survey application was created prior to a site visit in May 2022 in order to collect training and reference points for *Juncus*. The survey application was created through ArcGIS Survey 123 from ESRI. Records included species, GPS location, image, and commentary on surrounding marsh. Species were confirmed at multiple sites along Florida State Highway 65 near the northeastern boundary of the study area along with other sites along Apalachicola Bay (Figure 1). Though the number of samples was small (n=8), there were sufficient samples to identify the spectral profile of *Juncus* in the Landsat images. The field-collected sample points were compared to 1m spatial resolution imagery from the National Agriculture Imagery Program (NAIP) to increase the number training samples (pixels) for image classification of the true color Landsat composite with included NDVI and NDWI bands. NAIP 1m orthoimagery is available back to 2003, however, the products do not cover all states within the United States each year, and some counties for Florida were unavailable for the years are

2004 to 2006. Given the growth pattern of the target species, using NAIP imagery that is a year over or under the given Landsat image year can be used to estimate *Juncus* extent in known locations. These were confirmed by the spectral profile signature. NAIP imagery from 2020 was accessed through ArcGIS Online (ESRI, 2022) coupled with the survey data for the marsh collected in May 2022 to create the training and test datasets. NAIP images for the earlier years were downloaded to estimate marsh extent and compare with the spectral profile of the *Juncus* points from 2022 to ensure the target class is accurate given a lack of ground reference data for the marsh in the previous years.

3.2.3 Data Processing

A spectral profile (Figure 4) was identified using the sample field points as input for pixel selection in the May 2022 Landsat imagery. These areas of *Juncus* marsh were delineated with use of high-resolution NAIP imagery alongside the Landsat imagery to approximate areas for each sample. The training data for the *Juncus* category was identified and delineated from aerial and satellite imagery using ortho-photomosaic interpretation (Lopes et al., 2020) with the spectral profile as a reference. Ortho-photomosaic interpretation refers to the interpretation of aerial images that have been altered to correct distortions in a photo caused by camera tilt, perspective, lens distortion, or topographic relief (Doggett, 2020) to extract specific land cover types of known locations for training and/or reference data. Three other categories were added to the training and test samples to facilitate comparison between the target class *(Juncus)* and other prominent landcover types in the study area. These categories include Water, Forest, and Other Herbaceous. The Other Herbaceous category included predominately other marsh vegetation cover outside of *Juncus* dominant marsh with minor inclusions barren land, pasture, and any existing developed landed such as roads.

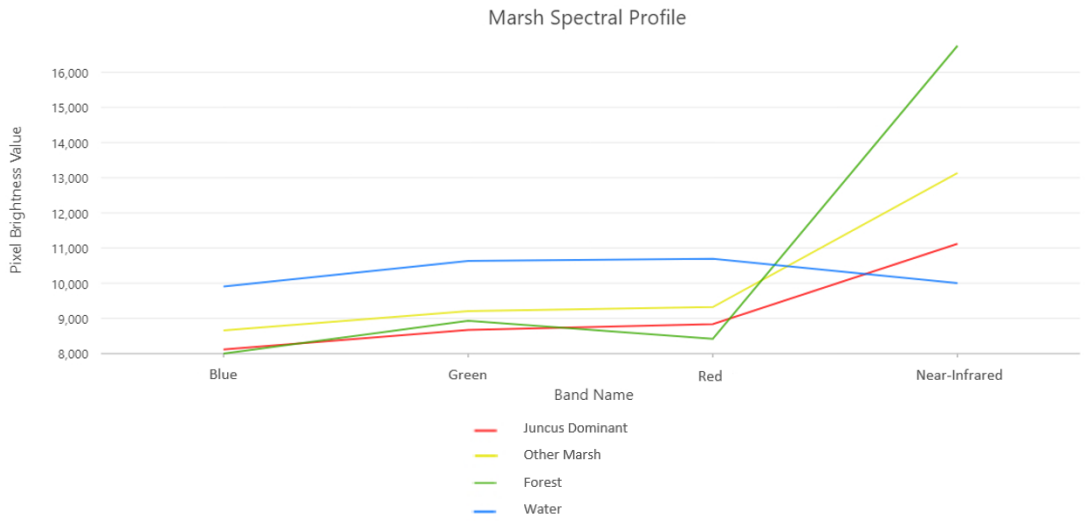

Figure 4. Spectral profiles of prominent landcover types in the study area, from Landsat Surface reflectance bands: The red represents the Juncus dominant marsh signature while the yellow represents marsh area with other mixed marsh vegetation, green line is forest cover and blue line is water.

Before performing maximum likelihood classification (MLC), two indices were created for each Landsat image to aid in distinguishing between vegetation cover types. These indices were Normalized Difference Vegetation Index (NDVI) and Normalized Difference Water Index (NDWI). Both indices have been shown to improve accuracy of marsh wetland classification (Vermote et al., 2016; Masek et al., 2006; Gao 1996). Indices for each year were computed using the raster calculate function within ArcGIS Pro (ESRI, 2020) and bands were generated for the NDVI and NDWI. The NDVI and NDWI bands were then combined with the natural color Landsat bands (Table 1) to create the input datasets for the MLC model.

NDVI uses the red band with the NIR band from the Landsat Surface Reflectance dataset collection to create a quantified vegetation greenness raster. This index is useful for understanding and visualizing vegetation density and plant vigor (Vermote, et al., 2016; Masek, et al., 2006). Below is the equation for the NDVI calculation:

$$NDVI = \frac{(NIR - Red)}{(NIR + Red)}$$

The NDWI is derived using the green band and the SWIR instead of the red band and NIR band. This index creates a raster that quantifies vegetation liquid water from surrounding area using satellite data (Gao, 1996). Below is the equation for the NDWI calculation:

$$NDWI = \frac{(Green - SWIR)}{(Green + SWIR)}$$

3.2.4 Image Classification and Change Detection Analysis

In this study, Landsat datasets and derived input data were classified using a MLC and detection of changes were subsequently examined, using the MLC and Compute Change Detection toolsets in ArcGIS Pro (ESRI, 2022). The digitized training data (described in Section 2.2) were used to train the maximum likelihood classifier and separate test data (reference data) were used for conducting accuracy assessments. The workflow for this process is presented in Figure 5.

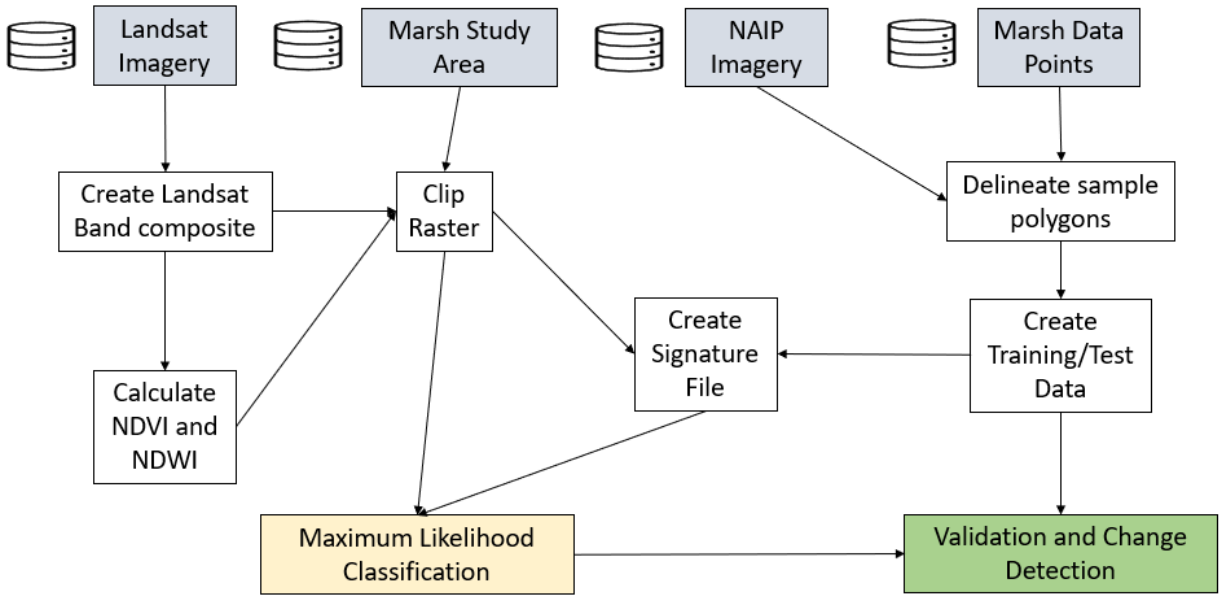

Figure 5. Workflow used to create, run, and validate the MLC results.

The training data for each of the years were used on the input rasters (described in Section 2.3) to create individual signature files (Figure 4). The signature files for each year of the input rasters were created, then used as input signature files for the MLC with the corresponding image. The test sample data were generated from a portion of the delineated *Juncus* sample polygons, to compute 250 points within the study area that are assigned a location and its corresponding class type. The class type for the resulting points were compared with the classified image results. An accuracy assessment was conducted using the reference data generated in the previous step to create a confusion matrix for each classified image. A confusion matrix compares the pixel values assigned by the classifier with reference data in order to evaluate the accuracy of a classified image. The matrices computed for the classified images included the overall classifier accuracy and kappa coefficient value along with omission and commission errors. The kappa coefficient is a measure of agreement between the classified values and their respective true values beyond chance assignment, 1 represents 100% agreement

and 0 represents no agreement. The user accuracy refers to the probability that a value was predicted to be in a class that it truly belongs to (correctly predicted values divided by the total number of values predicted). Producer accuracy is the probability that a value in a certain class was classified correctly. Commission errors refer to false positives in classes in the user accuracy, meaning values were predicted in a class in which they did not belong. A high commission error is a result of an overestimation of a class by the classification, or inclusion of values that are not the same as the ground truth. Omission errors refer to false negatives in the producer accuracy, meaning values that should have been predicted in a certain class were left out. A high omission error is the result of an underestimation of a class by the classification, or that ground truth points of class were excluded. All confusion matrices and error tables (Tables 2, 3, and 4) were calculated using ENVI imagery processing software (L3Harris Geospatial Solutions, Inc., 2022). After obtaining the classified images for each year, a change detection was then analyzed between 2008-2014 classified images and 2014-2022 classified images. The resulting feature classes were then reclassified in order to distinguish between gains (other classes to the *Juncus* class) and losses (*Juncus* class to one of the other classes). This information was compiled into a table to display the accumulative changes between years.

3.3 Results

3.3.1 Image Classification

Three classified images were produced during this study (Figure 6). Each of the classified images shows a discrete wetland composite, with distinct shifts in *Juncus* cover between years with 2014 showing the highest percentage of *Juncus* present. All three classified images yielded an overall accuracy of more than 94% and all Kappa values were over 0.9. This indicates that output had good agreement between classes in each classified image and the ground truth points

(reference points). Especially, the 2008 classified image had an overall accuracy of 94.2% and a Kappa coefficient of 0.92. The 2014 classified image had an overall accuracy of 98.3% and a kappa of 0.97. The 2022 classified image had an overall accuracy of 96.0% and a kappa of 0.94.

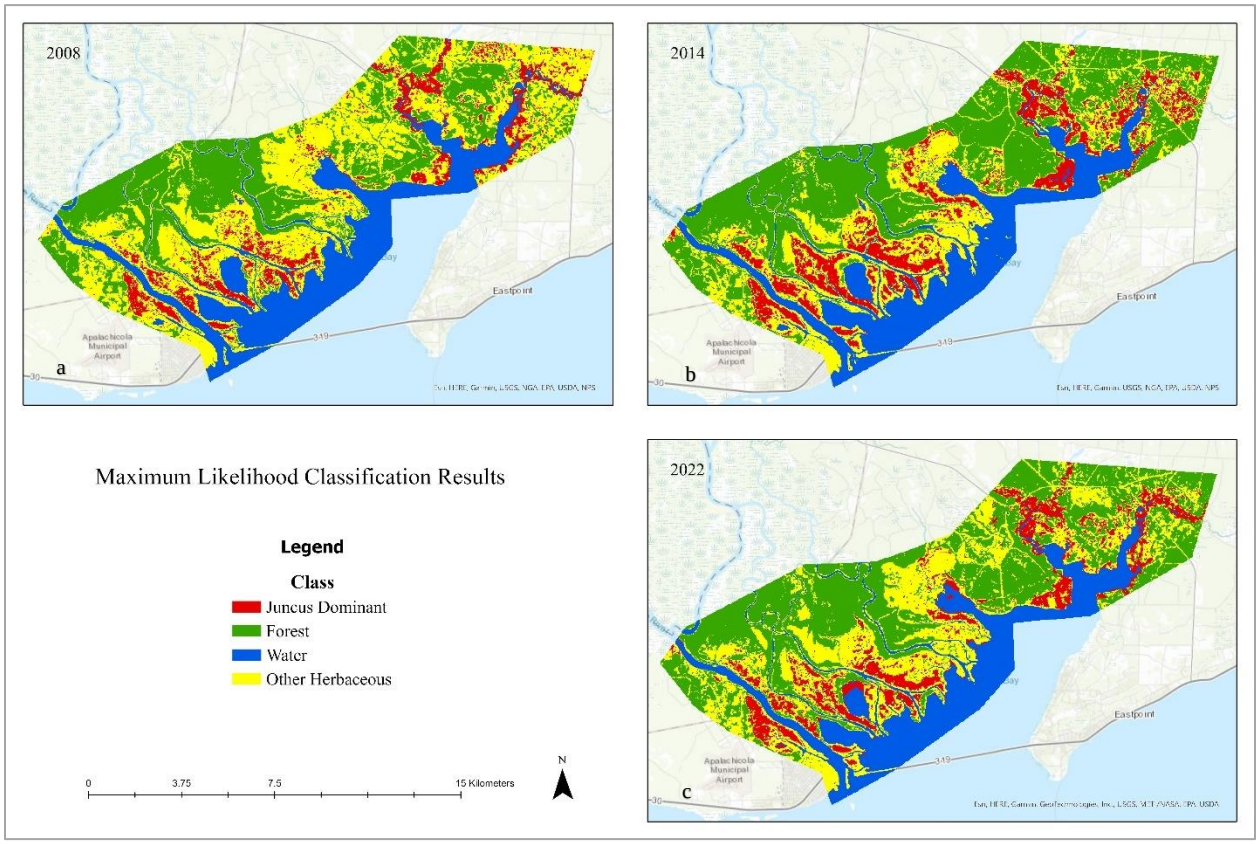

Figure 6. Landsat classified image results for 2008 (a), 2014 (b), and 2022 (c). Each image used for the MLC model were composed of the Blue, Green, Red, NDWI and NDVI bands

Pixels in the Forest, Water and Other Herbaceous category of the 2008 classified image, and Water and Other Herbaceous categories of the 2014 classified image were misclassified as *Juncus* for these two years, leading to an omission error of 27.0% and 12.6%, respectively (Tables 2 and 3). Error caused by confusion with the Other Herbaceous category in 2022 classified image was also seen, however, it was the lowest of the three: 10.2% (Table 4). The highest commission error was seen in the *Juncus* category in the 2022 classified image: 34.33% (Table 4), caused by pixels included in the *Juncus* category that belonged to the Other

Herbaceous category. The second highest commission error is in the Other Herbaceous category of the 2008 classified image: 19.12% (Table 2). This error was caused by inclusion of pixels from the Other, Water, and Forest categories within the *Juncus* class (Table 2).

Table 2. Confusion matrix for the 2008 classified image. This table contains the omission and commission errors between classes as well and the accuracy of each class. Overall accuracy was 94.2% with a Kappa coefficient of 0.9194.

2008	**Ground Truth (Percent)**						
Classes	***Juncus***	**Forest**	**Water**	**Other Herb.**	**Total**	**User Accuracy**	**Commission**
Unclassified	0.0	0.0	0.0	0.0	0.00		
Juncus	73.0	0.0	0.5	0.0	11.7	98.5	1.5
Forest	2.9	96.7	0.3	0.0	29.9	98.2	1.8
Water	4.6	0.0	98.5	0.0	35.5	98.0	2.0
Other Herb.	19.5	3.3	0.8	100.0	22.8	80.9	19.1
Total	100.0	100.0	100.0	100.0	100.0		
Producer Accuracy	73.0	96.7	98.5	100.0			
Omission	27.0	3.3	1.5	0.0			

Table 3. Confusion matrix for the 2014 classified image. This table contains the omission and commission errors between classes as well and the accuracy of each class. Overall accuracy was 98.3% with a Kappa coefficient of 0.9730.

2014	**Ground Truth (Percent)**						
Classes	***Juncus***	**Forest**	**Water**	**Other**	**Total**	**User Accuracy**	**Commission**
Unclassified	0.0	0.0	0.0	0.7	0.1		
Juncus	86.8	0.0	0.4	0.0	8.0	97.9	2.1
Forest	0.0	100.0	0.0	0.0	33.8	100.0	0.0
Water	1.3	0.0	99.2	0.7	48.6	99.7	0.3
Other Herb.	12.0	0.0	0.5	98.6	9.5	86.2	13.8
Total	100.0	100.0	100.0	100.0	100.0		
Producer Accuracy	86.8	100.0	99.2	98.6			
Omission	13.2	0.0	0.8	1.4			

Table 4. Confusion matrix for the 2022 classified image. This table contains the omission and commission errors between classes as well and the accuracy of each class. Overall accuracy was 96.0% with a Kappa coefficient of 0.9428.

2022	**Ground Truth (Percent)**						
Classes	***Juncus***	**Forest**	**Water**	**Other**	**Total**	**User Accuracy**	**Commission**
Unclassified	0.0	0.0	0.0	0.0	0.00		
Juncus	89.8	0.0	7.02	2.11	8.0	65.7	34.3
Forest	0.0	98.9	0.0	1.1	31.8	98.9	1.1
Water	0.0	0.0	93.0	0.0	26.7	100.0	0.0
Other Herb.	10.2	1.1	0.0	96.8	33.6	97.2	2.8
Total	100.0	100.0	100.0	100.0	100.0		
Producer Accuracy	89.8	98.9	93.0	96.8			
Omission	10.2	1.1	7.0	3.2			

3.3.2 Change Detection

Based on the classified image maps, two change detection maps were created to quantify the area of *Juncus* cover change between 2008 and 2014, and between 2014 and 2022, using the classified images. To better view and interpret the results, the study area for change detection was reduced in size and centered around the Apalachicola River and East River (Figure 7 and 8). For each change detection, a categorical difference was selected as the means of producing the results seen in Figures 7 and 8. Of the categorical difference calculation, only 6 class type changes were kept for analysis: *Juncus* to all other classes and all other classes to *Juncus*. The calculated area of change for each category can be seen in Table 5. Between 2008 and 2014, there was approximately 596.3 ha *Juncus* marsh expansion (Table 5), primarily between the Apalachicola and East Rivers (Figure 7). Most *Juncus* expansion appears to be centered around the St Marks River (seen in Figure 7 to the northeast of the Big Bay). Approximately 144.7 ha of *Juncus* marsh cover was lost between 2008 and 2014 (Table 5) that appears to be distributed more evenly across the target area. Between 2014 and 2022, there was much more loss than gain (Table 6). Approximately 157.8 ha of *Juncus* marsh cover was gained while 371.4 ha were lost. Some of the gain in *Juncus* marsh is overestimated due to misclassified pixels in the 2022 classified image: Water classified as *Juncus* (Table 4; Figure 8). Between the two change detection images (2008-2014 and 2014-2022), 300.0 ha overlapped. Of the 596.3 has of gain in the 2008-2014 change detection image, 270.8 ha were lost in the 2014-2022 change detection image. In the 300.0 ha of overlap, there was also 23.0 ha of gained *Juncus* marsh extent in the 2014-2022 change detection image that was previously lost in the 2008-2014 change detection. Of the total 300.0 ha overlap in the change detections, only 6.2 ha remained the same. In the

change detection between 2008 and 2022 (Figure 9), there was a net loss of 200.7 ha and a net gain of 425.5 ha in *Juncus* dominant marsh in the marshlands of the Apalachicola Bay (Table 5).

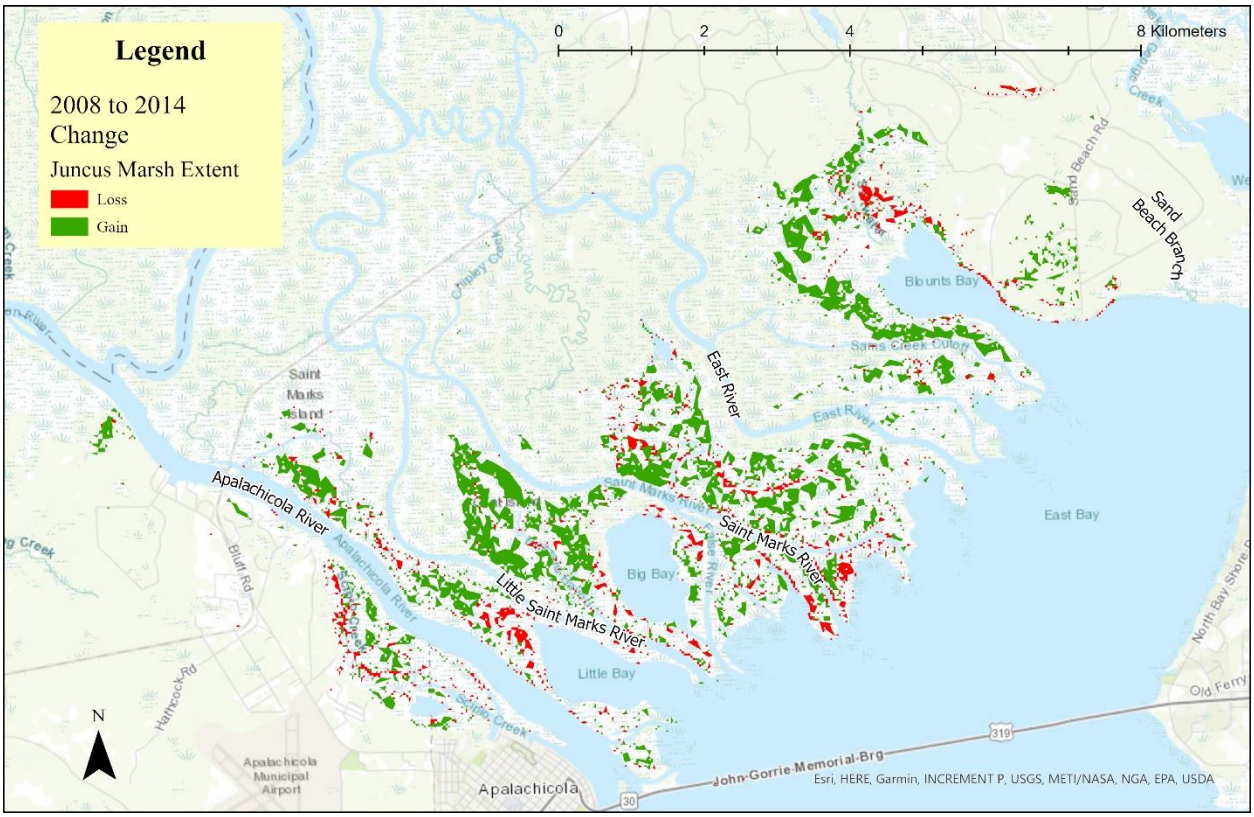

Figure 7. Map showing change in marsh extent between the 2008 classified image and the 2014 classified image. The red indicates loss of Juncus dominant marsh extent, and the green indicates gain of Juncus dominant marsh.

Change Detection between 2014 and 2022

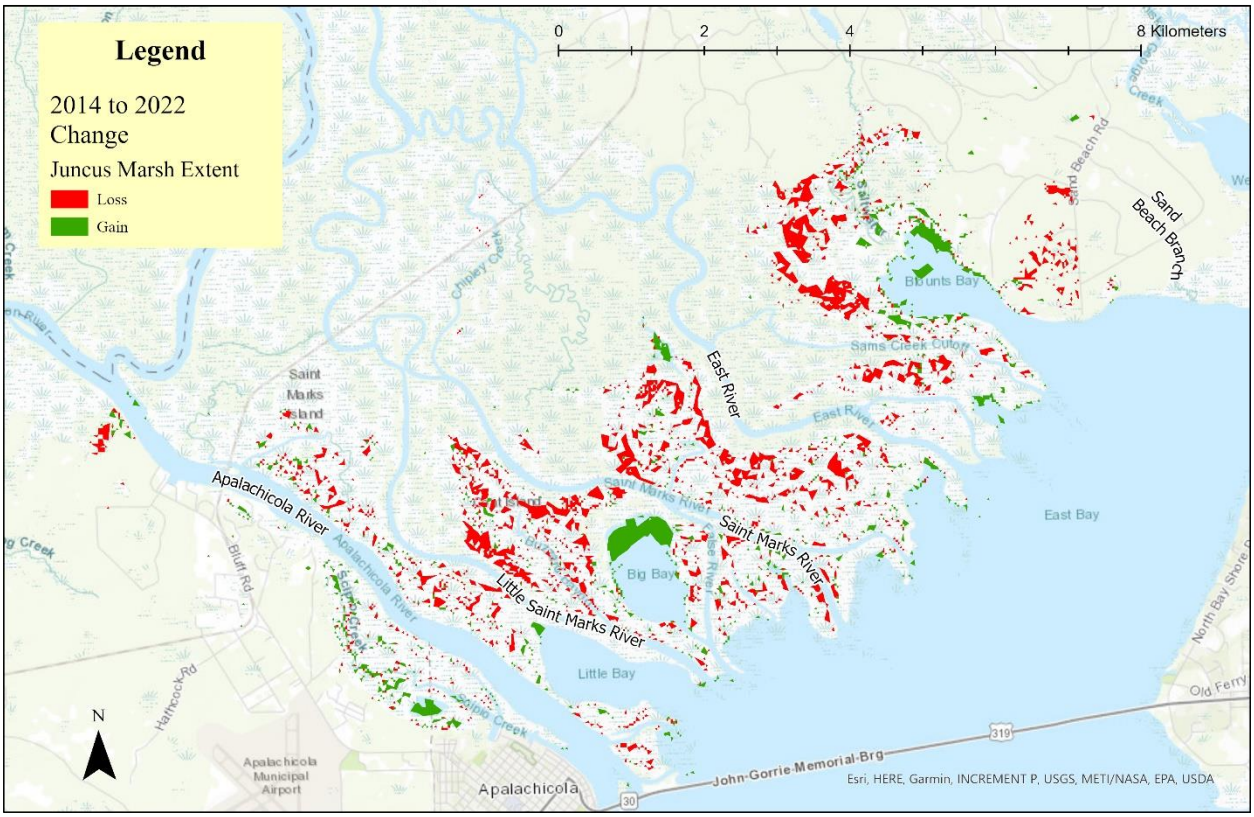

Figure 8. Map representing change observed between the 2014 classified image and the 2022 classified image. The red indicates loss of Juncus dominant marsh extent, and the green indicates gain of Juncus dominant marsh.

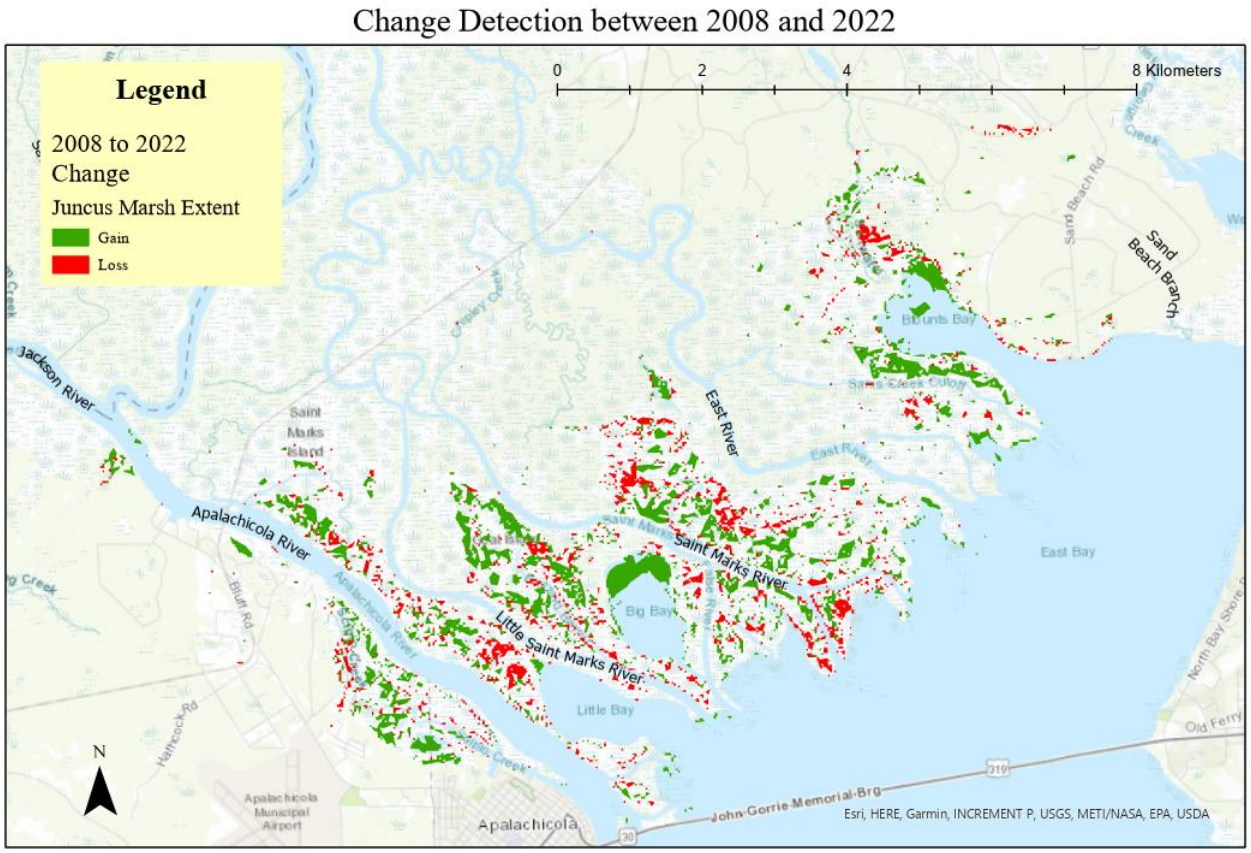

Figure 9: Map representing change observed between the 2008 classified image and the 2022 classified image. The red indicates loss of Juncus dominant marsh extent, and the green indicates gain of Juncus dominant marsh.

Table 5. This table represents the area (in has) of changes between any class and Juncus from 2008 to 2014, and 2014 to 2022. Total gained Juncus and total lost Juncus dominant marsh extents were added to the table for accumulative change in marsh extent.

	Class Change	**Change Detection Area in Hectares**					
		2008 - 2014	**Total**	**2014 - 2022**	**Total**	**2008 - 2022**	**Net Change**
***Juncus* Loss**	***Juncus* to Forest**	4.1	144.7	16.5	371.4	21.2	200.7
	***Juncus* to Water**	15.2		0.5		6.0	
	***Juncus* to Other**	125.4		354.4		173.5	
***Juncus* Gain**	**Forest to *Juncus***	12.4	596.3	1.3	157.8	1.5	425.5
	Water to *Juncus*	5.8		75.2		78.9	
	Other to *Juncus*	578.1		81.3		345.1	

3.4 Discussion

Although the omission and commission errors for the *Juncus* and Other Herbaceous classes in two of the three classified images (Tables 2 and 4) were higher than desired (15.0%), all classified images had an overall accuracy of 94.0% and higher with kappa values higher than 0.92. Similar accuracies have been found using MLC on other marshlands. A study by Zhang et al. (2020) performed MLC on images from 2012, 2013, 2014, and 2016 on Chongming Island, Shanghai, China. Their classified results yielded overall accuracies between 91.0%-94.0% and kappa values 0.82 and greater (Zhang et al., 2020). In another study of the marshes along the Pascagoula River, Mississippi where *Juncus* is also a dominant brackish and intermediate species, their classified results achieved between 98.9% and 99.7% overall accuracy for images from 1955, 1975, 1996, and 2014 (Waldron et al., 2021).

Errors in classification were likely due to the variation in color of the marsh given vegetation health and other indeterminant environmental factors. Variation in spectral properties of vegetation can be caused by a number of factors including, but not limited to, vegetation health, soil exposure, soil saturation, and mixture of species within a given pixel (30 x 30-meter grid cells). Confusion with water due to sediment loads can also occur. An example of this can be seen in the map of 2014-2022 change detection (Figure 8), where a section of the Big Bay (water) was misclassified as *Juncus*. Another example of this is also in Blounts Bay to the east, where an area in the middle of this bay was classified as *Juncus*. Much of the confusion was due to the various spectral properties of the vegetation although overall performance of the MLC results was satisfactory.

The multiple years of below-average Apalachicola River flows to the study area (Figure 3), especially with the amount of drought that occurred during this time interval, may have played an important role in the large increase in *Juncus* dominated marsh between 2008 and 2014 (Figure 7) due to the potential salinity increase as a result of decreased streamflow. Approximately 596.3 ha was gained, and 144.7 ha was lost (Table 5). Loss in *Juncus* dominant marsh was predominant due to conversion to other herbaceous marsh cover (125.4 ha between 2008 and 2014), followed by conversion to water and conversion to forest. In study by Waldron et al. (2021), they found a total loss of 1,072.8 ha in the Pascagoula River marshlands between 1955 and 2014, with 580.6 ha of marsh converted to water and 512.3 ha converted to forest. The gain of *Juncus* dominant marsh was predominantly due to conversion from other herbaceous class (578.1 ha between 2008 and 2014) (Table 5). Waldron et al (2021) found only 23.1 ha gain in marsh. Most increase in *Juncus* cover was centered around the St. Marks River between the Apalachicola and East Rivers. In a study conducted along the East River and the St. Marks River

(Celik et al., 2020), salinity along each river increases with proximity to the brackish water of the bay. However, the St. Marks River tends to have a higher average salinity (ranging from 0.02ppt – 12.7ppt mean daily salinity) than the East River (0.02ppt – 10.8ppt mean daily salinity) due to East River receiving additional freshwater input from creeks adjacent to the Apalachicola River system (Celik et al., 2020), which could contribute to the greater amount of increased *Juncus* cover between 2008 and 2014. This suggests that tidal connectivity could also contribute to the trend in *Juncus* growth along the main stem of the Apalachicola River.

Following the increase in average annual discharge of the Apalachicola River system between 2014 and 2022 (Figure 3), the area gained much less *Juncus* marsh cover than the previous time interval while the lost *Juncus* cover nearly doubled: approximately 157.8 ha gained, and 371.4 ha lost (Table 5) (Figure 8). This evidence continues to support that an increase in freshwater to the coastal wetland systems may affect *Juncus* marsh cover. However, when the change detection was performed between 2008 and 2022 (Figure 9), there was a net gain of 425.5 ha and net loss of 200.7 ha in *Juncus* dominant marsh. A study by Geselbracht et al. (2015) applied the Sea Level Affecting Marshes Model (SLAMM) to 6 major estuaries along the Florida Gulf of Mexico, including the Apalachicola River estuary, to predict changes in coastal wetlands out to the year 2100. They predicted there would be a net loss of 2,425 ha under a 1meter SLR in the Apalachicola River estuary. They also predicted there would be 10,503 ha increase in salt marsh, 7,834 ha increase in brackish marsh, and 2,303 ha increase in tidal freshwater marsh by the year 2100 under a 1meter SLR (Geselbracht et al., 2015).

Direct causes of this kind of shift in vegetation may vary, however, fluctuations in salinity can cause shifts in marsh growth patterns that allow for competitor species, in this case *Juncus*, to colonize areas further upriver with more freshwater species. With extreme climatic

events like drought, hurricanes, and SLR, coastal vegetation can experience large-scale changes relatively quickly (Mckee et al., 2004; Doyle et al., 2007). Contributing factors in changes to above ground biomass of salt marshes could be the amount of water input, vegetation composition, erosion, and more (Campbell &Wang, 2020). Droughts can also amplify this process when the fresh water supply to these coastal systems is decreased (DeSantis et al., 2007). One study concluded that an efficient means of protecting coastal marshes as well as their ecosystem services is through an integrated ecosystem-based management approach (Gedan et al., 2009). To develop an appropriate management plan for any system, understanding the ecosystem and its natural progression is important to making informed decisions. This study has addressed this lack of knowledge of the marsh extent near the Apalachicola region in the hopes of providing a methodology for monitoring changes to the marsh over time.

The use of remote sensing to detect *Juncus* communities along the lower Apalachicola River will allow for other monitoring applications. Due to the low elevation and slope of the Apalachicola region, there is potential for marsh migration inland as sea level rises, highlighting the importance of continued monitoring of coastal wetland systems. Recommendations for improving the accuracy of this analysis include the acquisition of additional field data for training and reference points within the study area. Limited field data (for marsh species) for training was supplemented with data from higher resolution imagery, however, this could have contributed to the errors observed in the classified image results. In order to address this issue in the future, an increased number of field samples for marsh species is required. For a more accurate assessment of the marsh, a revised study area with training data more focused around the mouth of the Apalachicola River would aid in removing uncertainty associated with some variation among the marsh vegetation. *Juncus* marshes in the lower river may have novel and

additional spectral profiles that were not present along the periphery of Apalachicola Bay where all training data was acquired. By limiting the environmental extent there are other factors such as mixed assemblages, phenology, and varied plant heights that may be missed and therefore some vegetation spectral variation (i.e., color) may be missed. Given the accuracy of the results despite the observed errors, this study provides an initial framework for continued monitoring of shifts in the Apalachicola marsh. The launch of the Landsat 9 satellite in 2021 could possibly provide future researchers with improved image quality that has the potential to increase the number of available remotely sensed images for assessment.

3.5 Conclusions

Image classification of Apalachicola marsh ecosystem and subsequent change detection analysis revealed a large increase in *Juncus* dominated marsh extent between 2008 and 2014, followed by a relatively large loss in *Juncus* dominant marsh between 2014 and 2022. When compared to the average annual river flow data (Figure 3), it appears that freshwater input plays a role in the marsh composition between more saline tolerant species (*Juncus*) and other marsh species (*Spartina* spp., *Cladium jamaicense*). Limitations of this study were the lack of a large input dataset for the marsh species from the lower river marshes, coarse spatial resolution for classification, and limited satellite imagery available for the initial time interval all of which possibly contribute to the errors observed in the classification. Even so, all three classified images yielded an overall accuracy of more than 94% and all Kappa values were over 0.92. Recommendations for improvements to this approach are as follows: (1) increase the number of field data points for the marsh and (2) finer spatial resolution than Landsat imagery.

References

Anderson, C. J., & Lockaby, B. G. (2011). Forested Wetland Communities as Indicators of Tidal Influence along the Apalachicola River, Florida, USA. *Wetlands*(31), 859-906. doi:https://doi.org/10.1007/s13157-011-0204-5

Baker, C., Lawrence, R., Montagne, C., & Patten, D. (2006, June). Mapping Wetlands and Riparian Areas Using Landsat ETM+ Imagery and Decision-Tree-Based Models. *WETLANDS, 26*(2), 465-474.

Brinson, M.M. and Christian, R.R. (1999, March). *Stability of Juncus roemerianus patches in a salt marsh*. Wetlands, 19(1), 65-70.

Campbell, A. D., & Wang, Y. (2020). Salt Marsh monitoring along the mid-Atlantic coast by Google Earth Engine enabled time series. *PLoS ONE, 15*(2). doi:10.1371/journal.pone.0229605

Celik, S., Anderson, C. J., Kalin, L., and Rezaeianzadeh, M. (2020). Long-term Salinity, Hydrology, and Forested Wetlands Along a Tidal Freshwater Gradient. Estuaries and Coasts, 44, 1816-1830. doi:10.1007/s12237-021-00977-8.

Correll, M. D., Hantson, W., Hodgman, T. P., Cline, B. B., Elphick, C. S., Shriver, W. G., Shriver, G., Tymkiw, E. L., and Olsen, B. J. (2019). Fine-Scale Mapping of Coastal Plant Communities in the Northeastern USA. *Applied Wetland Science,* 39, 17-28. doi:10.1007/s13157-018-1028-3

Crain, C.M., Silliman, B.R., Bertness, S.L., and Bertness, M.D. (2004). *Physical and biotic drivers of plant distribution across estuarine salinity gradients*. Ecology, 85(9), 2539-2549.

DeSantis, L. R., Bhotika, S., Williams, K., & Putz, F. E. (2007). Sea-level rise and drought interactions accelerate forest decline on the Gulf Coast of Florida, USA. *Global Change Biology*, *13*(11), 2349-2360. doi:10.1111/j.1365-2486.2007.01440.x

Doyle, T. W., O'Neil, C. P., Melder, M. P., From, A. S., & Plata, M. M. (2007). Tidal Freshwater Swamps of the Southeastern United States: Effects of Land Use, Hurricanes, Sea-level Rise, and Climate Change. *Ecology of Tidal Freshwater Forested Wetlands of the Southeastern United States*. doi:10.1007/978-1-4020-5095-4_1

Doggett, S. (2020). *What is an orthomosaic? Orthomosaic Maps & Orthophotos explained*. dronegenuity. Retrieved November 28, 2022, from https://www.dronegenuity.com/orthomosaic-maps-explained/

Edmiston, H. L. (2008). *A River Meets the Bay, The Apalachicola Estuarine System. Apalachicola National Estuarine Research Reserve. Apalachicola, FL. Retrieved from https://coast.noaa.gov/data/docs/nerrs/Reserves_APA_SiteProfile.pdf*

ESRI. (n.d.). About ArcGIS Pro-ArcGIS Pro | Documentation. Retrieved October 3, 2022, from https://pro.arcgis.com/en/pro-app/2.8/get-started/get-started.htm

ESRI. (2022, November). ArcGIS Online. Retrieved from https://www.arcgis.com/index.html

Field, D. W. (1991). *Coastal wetlands of the United States: An accounting of a valuable National Resource*. National Oceanic and Atmospheric Administration.

Gao, B.-c. (1996, December). NDWI—A normalized difference water index for remote sensing of vegetation liquid water from space. *Remote Sensing of Environment, 58*(3), 257*266. doi:10.1016/50034-4257(96)00067-3

Geselbracht, L.L., Freeman, K., Birch, A.P., Brenner, J., and Gordon, D.R. (2015). Modeled Sea Level Rise Impacts on Coastal Ecosystems at Six Major Estuaries on Florida's Gulf Coast: Implications for Adaptation Planning. *PLoS ONE,* 10 (7): e0132079. doi: 10.1371/journal.pone.0132079

Hackney, C.T., Brady, S., Stemmy, L., Boris, M., Dennis, C., Hancock, T., O'Bryon, M., Tilton, C., and Barbee, E. (1996, March). *Does intertidal vegetation indicate specific soil and hydrologic conditions*. Wetlands, 16(1), 89-94.

Harper, R. M. (1911). THE RIVER-BANK VEGETATION OF THE LOWER APALACHICOLA, AND A NEW PRINCIPLE ILLUSTRATED THEREBY. In *Source: Torreya* (Vol. 11, Issue 11).

L3Harris Geospatial Solutions, Inc. (n.d.). *Software & technology: ENVI*. L3Harris Geospatial. Retrieved October 3, 2022, from https://www.l3harrisgeospatial.com/Software-Technology/ENVI

Landsat Missions. (n.d.). *Landsat satellite missions*. Landsat Satellite Missions | U.S. Geological Survey. Retrieved August 21, 2022, from https://www.usgs.gov/landsat-missions/landsat-satellite-missions

Leitman, H. M., Sohm, J. E., and Franklin, M. A. (1983). Wetland hhydrology and tree distribution of the Apalachicola River floodplain, Florida. USGS Water Supply Paper 2196-A, 1-52.

Livingston, R. J. (1984). *The ecology of the Apalachicola Bay system: an estuarine profile.* Washington, D.C.: U.S. Department of the Interior.

Lockaby, B. G., Anderson, C. J., & Click, N. (2013). Chnages in Wetland Forest Structure, Basal Growth, and Composition across a Tidal Gradient. *The American Midland Naturalist, 170*(1), 1-13. doi:10.1674/0003-0031-170.1.1

Lopes, C. L., Mendes, R., Casador, I., & Dias , J. M. (2020, September). Assessing salt marsh extent and condition changes with 35 years of Landsat imagery: Tagus Estuary case study. *Remote Sensing of Environment, 247*, 111939. doi:10.1016/j.rse.2020.111939

Masek, J.G.; Vermote, E.F.; Saleous, N.E.; Wolfe, R.; Hall, F.G.; Huemmrich, K.F.; Gao, F.; Kutler, J.; and Lim, T. (2006) A Landsat surface reflectance dataset for North America, 1990-2000. IEEE Geoscience and Remote Sensing Letters 3(1), 68-72. doi: 10.1109/LGRS.2005.857030.

McKee, K. L., Mendelssohn, I. A., and Materne, M. D. (2004). Acute salt marsh dieback in the Mississippi River deltaic plain: a drought-induced phenomenon? *Global Ecology and Biogeography*, 13, 65-73. doi: 10.1111/j.1466-882X.2004.00075.x

Mitsch, W. J., & Gosselink, J. G. (2015). *Wetlands* (Fifth ed.). Hoboken, New Jersey: John Wiley & Sons, Inc.

NOAA Fisheries. (2022, February 4). *Coastal Wetland Habitat*. NOAA. Retrieved April 30, 2022, from https://www.fisheries.noaa.gov/national/habitat-conservation/coastal-wetland-habitat#:~:text=Coastal%20wetlands%20support%20important%20benefits,for%20commercial%20and%20recreational%20fisheries.

Ramsey III, E. W., and Rangoonwala, A. (2004). Remote Sensing and the Optical Properties of the Narrow Cylindrical Leaves of *Juncus Roemerianus*. IEEE Transactions on Geoscience and Remote Sensing, 42(5). doi:10.1109/TGRS.2003.823283

Ramsey III, E. W., Sapkota, S. K., Barnes, F. G., and Nelson, G. A. (2002). Monitoring the recovery of *Juncus* roemerianus marsh burns with the Normalized Difference Vegetation Index and the Landsat Thematic Mapper data. Wetlands Ecology and Management, 10, 85-96.

Stout, J.P. (1984). *Ecology of irregularly flooded salt marshes of the northeastern Gulf of Mexico: a community profile*. United States.

Touchette, B.W., Smith, G.A., Rhodes, K.L., and Poole, M. (2009, April). Tolerance and avoidance: *Two contrasting physiological responses to salt stress in mature halophytes Juncus roemerianus Scheele and Spartina alterniflora Loisel*. Journal of Experimental Marine Biology and Ecology. 380, 106-112. Doi: 10.1016/j.jembe.2009.08.015

Townend, I., Fletcher, C., Knappen, M., and Rossington, K. (2011). *A review of salt marsh dynamics*. Water and Environment, 25, 477-488. doi:10.1111/j.1747-6593.2010.00243.x

U.S. Department of the Interior. (2022). *What are the best Landsat spectral bands for use in my research? | U.S. Geological Survey*. https://www.usgs.gov/faqs/what-are-best-landsat-spectral-bands-use-my-research#faq

U.S. Department of Agriculture. (n.d.). *Natural Resources Conservation Service*. Coastal Wetland Definitions | NRCS Plant Materials Program. Retrieved August 21, 2022, from https://www.nrcs.usda.gov/wps/portal/nrcs/detail/plantmaterials/technical/publications/?cid=stelprdb1044268

U.S. Fish & Wildlife Service. (2022, April 28). *National Wetlands Inventory*. National Wetlands Inventory | U.S. Fish & Wildlife Service. Retrieved April 30, 2022, from https://www.fws.gov/program/national-wetlands-inventory

Vermote, E., Justice, C., Claverie, M., & Franch, B. (2016). *Preliminary analysis of the performance of the Landsat 8/OLI land surface reflectance product.* Remote Sensing of Environment, 185, 46-56.

Waldron, B., Claire, M., Carter, G. A., & Biber, P. D. (2021). Using Aerial Imagery to Determine the Effects of Sea-Level Rise on Fluvial Marshes at the Mouth of the Pascagoula River (Mississippi, USA). *Journal of Coastal Research, 37*(2), 389-407. Retrieved from https://doi.org/10.2112/JCOASTRES-D-20-00037.1

Yang, X., Zhu, Z., Qiu, S., Kroeger, K. D., Zhu, Z., & Covington, S. (2022, July). Detection and characterization of coastal tidal wetland change in the northeastern US using Landsat time series. *Remote Sensing of Environment, 276*, 113047. doi:10.1016/j.rse.2022.113047

Zhang, X., Xiao, X., Wang, X., Xu, X., Chen, B., Wang, J., . . . Li, B. (2020, September). Quantifying expansion and removal of Spartina alterniflora on Chongming island, China, using time series Landsat images during 1995–2018. *Remote Sensing of Environment, 247*, 111916. doi:10.1016/j.rse.2020.111916

Chapter 4 - Conclusion

For years, the Apalachicola National Estuarine Research Reserve (ANERR) has been used for studies examining many different components of wetland communities and the biophysical attributes that contribute to different functions within this ecosystem. The overall goal of this thesis was to better understand the composition of Apalachicola coastal wetland types: freshwater forested wetlands and marshes specifically. Two primary objectives were designed to meet this overall goal, with each developed as a standalone study.

The first primary objective of this work was to use the National Aerial Imagery Program (NAIP) 1-meter imagery to assess the extent of the tidal freshwater forested wetland (TFFW) communities along the lower Apalachicola River floodplain using detection of an indicator species (cabbage palm – *Sabal palmetto*) for one of the two community types of TFFW. The most accurate output had an overall accuracy of Texture classified image (red, green, blue, NIR, and NIR variance texture band) (kappa =0.83), and user and producer accuracies for cabbage palm were 88.7% and 94.0%, respectively. Based on this product, cabbage palm was observed to be present through the entire extent of the study area. Dense stands were detected along river edges and the largest detected stand of cabbage palm detected directly above the marsh lining the Apalachicola Bay. Additionally, findings suggest that NDVI had a negative impact on the detection of cabbage palm in leaf-off imagery. Though a discrete tidal/nontidal boundary was not detectable using cabbage palm, outcomes from this work can facilitate monitoring of TFFWs in the Apalachicola floodplain as well as promote informed mitigation practices and aid in planning for future land management in the face of sea level rise. Recommendations for future work to improve the classification accuracy include: 1) limiting the study area strictly to the Apalachicola

River floodplain to limit confusion with pine and 2) incorporate high-resolution canopy height models.

The second primary objective of this was to assess changes in the Apalachicola marshlands over the past 14 years. To do this, the spatial extent of *Juncus roemerianus* in Apalachicola, Florida was assessed using Landsat imagery and a time series analysis was performed. This was accomplished by performing an image classification using Landsat images from 2008, 2014, and 2022 (overall accuracy of 94.2%, 98.3%, and 96.0%, repsectively) to detect a dominant brackish marsh species (black needlerush – *Juncus roemerianus*). A change detection was then performed between 2008 and 2014, and 2014 and 2022. Between 2008 and 2014, there was a net gain of 451.6 ha in the *Juncus* class whereas the years between 2014 and 2022 experienced a net loss of 213.6 ha in *Juncus*. When compared with the average annual river flow between 2008 and 2022, it appears that freshwater input from the Apalachicola River plays a role in marsh composition and could be impacting the gain/loss of the *Juncus* marsh over time. Limitations of this study were the lack of a large input training dataset for the marsh species (particularly from within the river marshes), coarse spatial resolution of input imagery, and limited satellite imagery available for the initial time interval (2000-2022), all of which possibly contributed to errors in the classification. Even so, 94.0% overall accuracy was achieved for the three classified images. Recommendations for improving this approach include: 1) increase the number of field data points for the marsh species and 2) finer spatial resolution than Landsat imagery.

Considering findings from both studies and the overall goal of the thesis, the spatial extent of Apalachicola's wetland communities has been successfully represented. Though cabbage palm appears to have a broader extent than expected within the Apalachicola River

floodplain, its spatial extent could be utilized along the lower reach of the Apalachicola River floodplain to track changes in the TFFW/marsh transition over time. These findings also highlight the importance of the NIR variance band in cabbage palm detection, specifically. The marshlands of this area have experienced a change in composition over the last 14 years, which has previously been unknown. The latest known information regarding the Apalachicola marshlands and their spatial extent came from 2008, with most of the species information dating back to the 1990s and older. This study fills the gap between 2008 and 2022 on the spatial extent of Apalachicola marsh and presents an approach for continued monitoring for the Apalachicola River floodplain.